



A comprehensive review of tsunami and palaeotsunami research in Chile

Tomás León^{a,*}, A.Y. Annie Lau^a, Gabriel Easton^b, James Goff^{c,d}

^a School of Earth and Environmental Sciences, The University of Queensland, St Lucia 4072, Brisbane, Australia

^b Departamento de Geología, Facultad de Ciencias Físicas y Matemáticas, Universidad de Chile, Plaza Ercilla 803, Santiago, Chile

^c Earth and Sustainability Science Research Centre, School of Biological, Earth and Environmental Sciences, University of New South Wales, Sydney 2052, Australia

^d School of Ocean and Earth Science, Faculty of Environmental and Life Sciences, University of Southampton, UK

ARTICLE INFO

Keywords:

Chile
Tsunami deposits
Palaeotsunami
Orphan tsunamis
Criteria

ABSTRACT

Chile is a tsunami-prone country. Since the 1960 Chilean earthquake triggered a Pacific-wide tsunami, there has been a considerable amount of research conducted on the geologic evidence for tsunamis along the coast of Chile. This review aims to gather all the evidence of tsunami inundation to identify which areas along the coast of Chile have been affected during modern, historical, and prehistoric times. This contributes to assessing the local and regional impacts of past events and helps to identify potential sites for further study. We seek to show the spatial and temporal distribution of tsunami deposits affected by their preservation in different climate zones. We also seek to assess the interpretation of each deposit by comparing information provided from a variety of sources and analyses. The review shows that thirty-one tsunamigenic events have been reported in historic times from 1570 CE to 2015 but deposits have only been found for twelve of these. There are ninety-two palaeotsunami deposits along Chile's coast and these span from the Miocene to Late Holocene. Geological evidence has been reported from fifty-seven sites of which 70% were found in southern Chile. While many deposits were identified in coastal lakes and river floodplains in southern Chile, tsunami deposits in the north are more commonly found on coastal plains, clifftops, and marshes. We also created a table assigning a level of certainty for each deposit. This is developed by the consideration of five criteria that include the use of multiproxy analyses, the correlation of a site with other deposits, comparisons with numerical simulations or historic counterparts, discrimination of the deposit from other possible processes, and a critical evaluation of the data in the original publication. This work provides insight into the types of environments that are most likely to contain evidence of past tsunamis and highlights the potential of finding more evidence in Chile of Pacific-wide "orphan tsunamis," such as the 1420 CE event that inundated the coast of Japan. Altogether, this review reveals a high frequency of tsunamis on the Chilean coasts and indicates that in some areas ancient tsunamis have reached higher inundations than those reported in the historic record, therefore, these data should be considered in future tsunami modelling to be better prepared for future events.

1. Introduction

In the past decade, research on catastrophic marine inundation events has brought remarkable advances in tsunami hazard assessment and management. These advances have enhanced the study of modern, historical and palaeotsunamis, emphasizing the use of multidisciplinary approaches to affirm interpretations of deposits and draw improved conclusions about tsunami hazards. This progress is rewarding for those countries where coastal populations are gradually increasing and are frequently affected by tsunamigenic events. Chile is one of these countries, located adjacent to the Perú-Chile Trench where the Nazca Plate is

subducting beneath the South America Plate at an approximate rate of 67 mm/yr. (Schurr et al., 2014), while to the south, the Antarctic Plate is subducting at a rate of 18.5 mm/yr. (Moreno et al., 2011) (Fig. 1). The country has been affected by numerous large earthquakes, over 8.0 Mw, during historical times such as the 8.7–8.9 Mw event in Iquique in 1877 CE, 8.8 Mw El Maule in 2010 and the largest earthquake ever recorded, the 9.5 Mw Valdivia in 1960 (Ruiz and Madariaga, 2018). All these events triggered large tsunamis affecting Chilean coasts as well as far-field countries across the Pacific such as Hawaii, New Zealand, and Japan (e.g., Shuto and Fujima, 2009; Donnelly et al., 2017; Chagué et al., 2018). In addition to the historical tsunamis recorded in Chile,

* Corresponding author.

E-mail address: t.leoncortes@uq.edu.au (T. León).

<https://doi.org/10.1016/j.earscirev.2022.104273>

Received 7 April 2022; Received in revised form 15 November 2022; Accepted 25 November 2022

Available online 2 December 2022

0012-8252/© 2022 Elsevier B.V. All rights reserved.

there is also evidence of ancient events for which there are no historical records or written observations (palaeotsunamis) (e.g., León et al., 2019; Abad et al., 2020). These have been identified by geological studies of onshore environments along the length of Chilean coasts.

Tsunami deposits are physical evidence of these events and provide critical information to quantify the proportion of present and past tsunamis. The study of tsunami deposits allows researchers to identify physical processes involved, such as hydraulic settings (i.e., flow velocity), sediment sources, modes of transport, the extent of flooding, and many others (e.g., Costa et al., 2020). In Chile, tsunami deposits range from mud layers cutting the normal stratigraphy in coastal lakes (e.g. Kempf et al., 2017; Kempf et al., 2020) or shallow marine platforms (e.g., Vargas et al., 2005), through sand layers between archaeological (e.g., León et al., 2019; Muñoz Cupitty, 2019)) and wetland layers (e.g., Cisternas et al., 2012; DePaolis et al., 2021; Hocking et al., 2021; Araya et al., 2022; Easton et al., 2022), to boulder fields on coastal cliffs (e.g., Abad et al., 2020) and coastal plain (e.g., Bahlburg et al., 2018; Spiske et al., 2020)). It should be noted that some studies have helped define the limits of tsunami inundation and, in some cases, have indicated that

palaeotsunamis reached higher run-ups than their historical counterparts, occurring numerous times in the past (e.g., León et al., 2019; Abad et al., 2020; DePaolis et al., 2021; Salazar et al., 2022). Consequently, tsunami deposits are a crucial source of information in helping to understand the magnitude and frequency of past events in different areas of Chile.

Therefore, a comprehensive compilation of tsunami and palaeotsunami deposits in Chile denotes a valuable contribution to evaluating tsunami impacts along the coast of Chile. Recently, Goff et al. (2020) synthesised palaeotsunami data from around the Sino-Pacific region providing a broad spatial and temporal scale and estimating magnitude and frequency. While the paper summarised evidence from Chile, it only looked at palaeotsunami research done after 2011, and a comprehensive review of all tsunami studies is still needed. Furthermore, no qualitative assessments of the criteria for relating individual deposits to a tsunami or palaeotsunami event have been carried out.

Through a systematic review of journal articles, scientific reports, books, and research theses, this paper aims to: (1) identify all historical earthquakes that triggered tsunamis in Chile, (2) map the spatial and

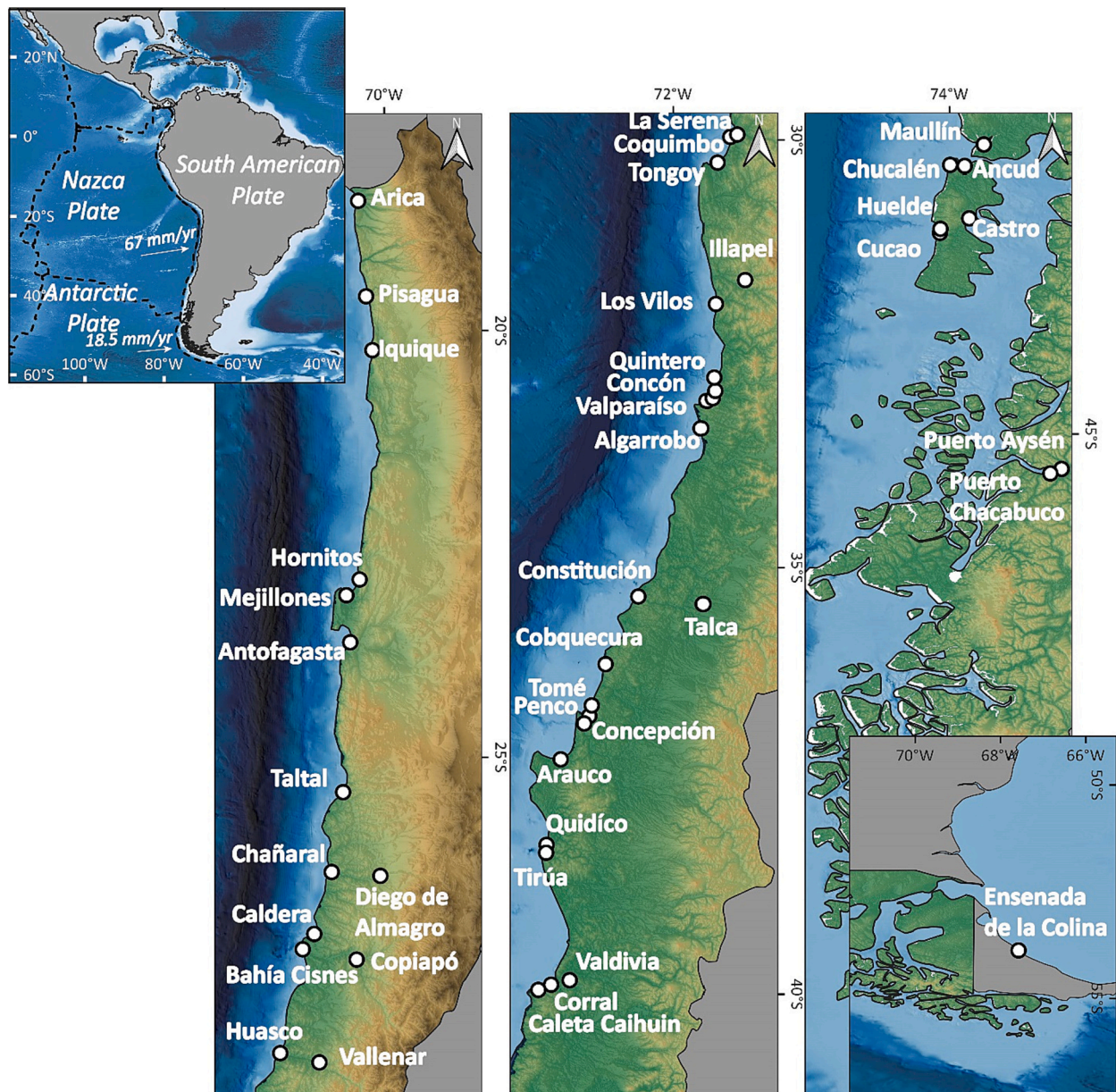


Fig. 1. General tectonic background, main cities and localities of Chile mentioned in the text.

temporal distribution of tsunami deposits, (3) identify the granulometry of the deposits, (4) explore how climatic control on sediment preservation may affect the distribution of tsunami deposits, (5) scale the confidence of the deposit according to the amount of information that supports a tsunami interpretation, (6) study the absence of sedimentary deposits from some historical tsunamis, and (7) highlight areas with a lack of data and outline a series of key research questions to help define future research priorities within Chile.

To achieve these aims, this article first describes studies relevant to tsunamis in Chile. Second, a discussion of tsunami deposit characteristics and the significance of the environment to the geological record and preservation potential is presented. Third, this review assesses the significance of these records to tsunami hazards in Chile and poses new questions that might direct future research priorities in the region.

2. Methods: A systematic review and the tsunami deposit criteria assessment

This work reviewed published articles that described modern, historical, and prehistoric tsunami events. The information was selected according to the reliability of the evidence and is gathered in Table 3. Each deposit is described according to its physical characteristics, the age of the event, the depositional environment, and the proxies that support a tsunami interpretation.

2.1. The structure of this review

We used three rules to construct this review. First, the interpretations considered all tsunami deposits, including modern, historical and palaeotsunami evidence, reported in the literature to present a complete temporal and spatial distribution of events recorded in Chile.

Second, the tsunami deposit count is based on the interpretation of each report. Each layer is counted as a separate tsunami deposit. If a deposit related to the same tsunami is identified at multiple locations, it is considered the same event. However, if different studies recorded deposits from an event at the same location, they are counted separately. In the case of boulders, if multiple boulders were transported by the same event and were reported in the same study, they are counted as a single deposit.

Finally, this work analysed the proxies used to interpret tsunamigenic layers in each article. Therefore, statistical analyses of the proxies are based on the number of articles and not the number of deposits. Also, the assignment of each proxy category was based on the proxy toolkit for palaeotsunami deposits as presented by Goff et al. (2012b).

2.2. Tsunami databases used

In Chile, earthquakes occur both under the sea and continent, so not all events trigger tsunamis. For this reason, the first step is to identify historic events that triggered tsunamis in Chile. This investigation reviewed the local and regional seismic databases of South America (e.g., CERESIS, 1985a, 1985b), articles concerning major earthquakes in Chile (e.g., Lomnitz, 1970; Comte and Pardo, 1991; Lomnitz, 2004; Ruiz and Madariaga, 2018) and information from government agencies such as the Servicio Hidrográfico y Oceanográfico de la Armada de Chile (SHOA) and the Centro Sismológico Nacional of the University of Chile (CSN). Additionally, information from the National Centers for Environmental Information/ World Data Service (NCEI/WDS) Global Historical Tsunami Database was used to add more details of tsunamigenic events, but also to include records missing from other sources (National Oceanic and Atmospheric Administration, 2022). NOAA defines a “Tsunami Event Validity” to assess the occurrence of tsunamis based on the report. Due to the wide range of the NCEI/WDS dataset, some records are questionable, so we opted to only include events that have high validity scores (3 and 4) in our list of historic tsunamigenic events in Chile (Table 1).

Table 1

Six criteria for the tsunami deposit confidence level assessment. More “yes” indicate the deposit is more likely a tsunami deposit.

Criterion	YES	NO
C1. Does the tsunami interpretation include both physical (includes geological, chemical, biological and geomorphological) and cultural (include archaeological, anthropological e.g., oral history and written records, and contextual e.g., local knowledge of tsunamigenic source) evidence?	<ul style="list-style-type: none"> Both disciplines are met 	<ul style="list-style-type: none"> Only one discipline is met.
C2. Can this deposit be correlated with other deposits from the same/ other articles to suggest a tsunami origin?	<ul style="list-style-type: none"> Deposits are correlated with others from other areas. 	<ul style="list-style-type: none"> No correlation with other deposits
C3. Is there any historic counterpart of numerical model to validate the tsunami-origin at the deposit's location?	<ul style="list-style-type: none"> Historic records mentioning an event in the area or numerical simulations that match the deposit location. 	<ul style="list-style-type: none"> Neither historic nor numerical simulations.
C4. Have other mechanisms of marine inundation been considered in the original research?	<ul style="list-style-type: none"> Description and discussion about similar events, to confirm or discard tsunami origin. 	<ul style="list-style-type: none"> Alternative interpretation has not been mentioned.
C5. Is the deposit deemed a tsunami deposit with corroborating evidence?	<ul style="list-style-type: none"> Comments of the authors on the confidence of the interpretation. 	<ul style="list-style-type: none"> No comments about the level of confidence.

2.3. Categorise tsunami deposits according to the locations' climatic macrozones

Due to its wide latitudinal range, Chile has a rich environment diversity that is influenced by the Pacific Anticyclone and the Humboldt Current, and the combination of morphological elements, such as the Andes Mountains and the Coast that give it its characteristics in terms of relief, natural vegetation, and soils. Therefore, we chose to use the division of (Ministerio de Obras Públicas, 2015), which classifies the country into four macro zones based on geographic, hydrographic, and climatic similarities (Fig. 2). From north to south, the North macrozone covers an area of 300,900 km² where 12.67% of the population lives. It is characterized by a dry and warm climate with an average of ~20 °C and 87 mm/year of rainfall. To the south of this, the Central macrozone shows lower temperatures (~17 °C), but higher rainfall with an average of 943 mm/year. This is the most populated area with 61.65% of the population in an area of 78,482 km². Next, the Southern macrozone is one of the most humid with 2420 mm/year of average precipitation and 12 °C of temperature. Here lives 24.16% of the population in an area of 135,925 km². Finally, the Austral zone covers 240,791 km² where only 1.52% of the population lives. The climatic conditions are characterized by a temperature of 10 °C and 2963 mm/year of precipitation. These four macrozones have climatic variations from west to east, but since the objective of this work is the study of tsunami deposits, only coastal variations were considered throughout the discussion, based on the classic climate classification of Köppen-Geiger modified by Peel et al. (2007) (Fig. 2). The benefit of this approach is that it allows a consideration of the climatic conditions in which tsunami deposits are preserved allowing us to compare the type of deposits found in different climate macrozones.

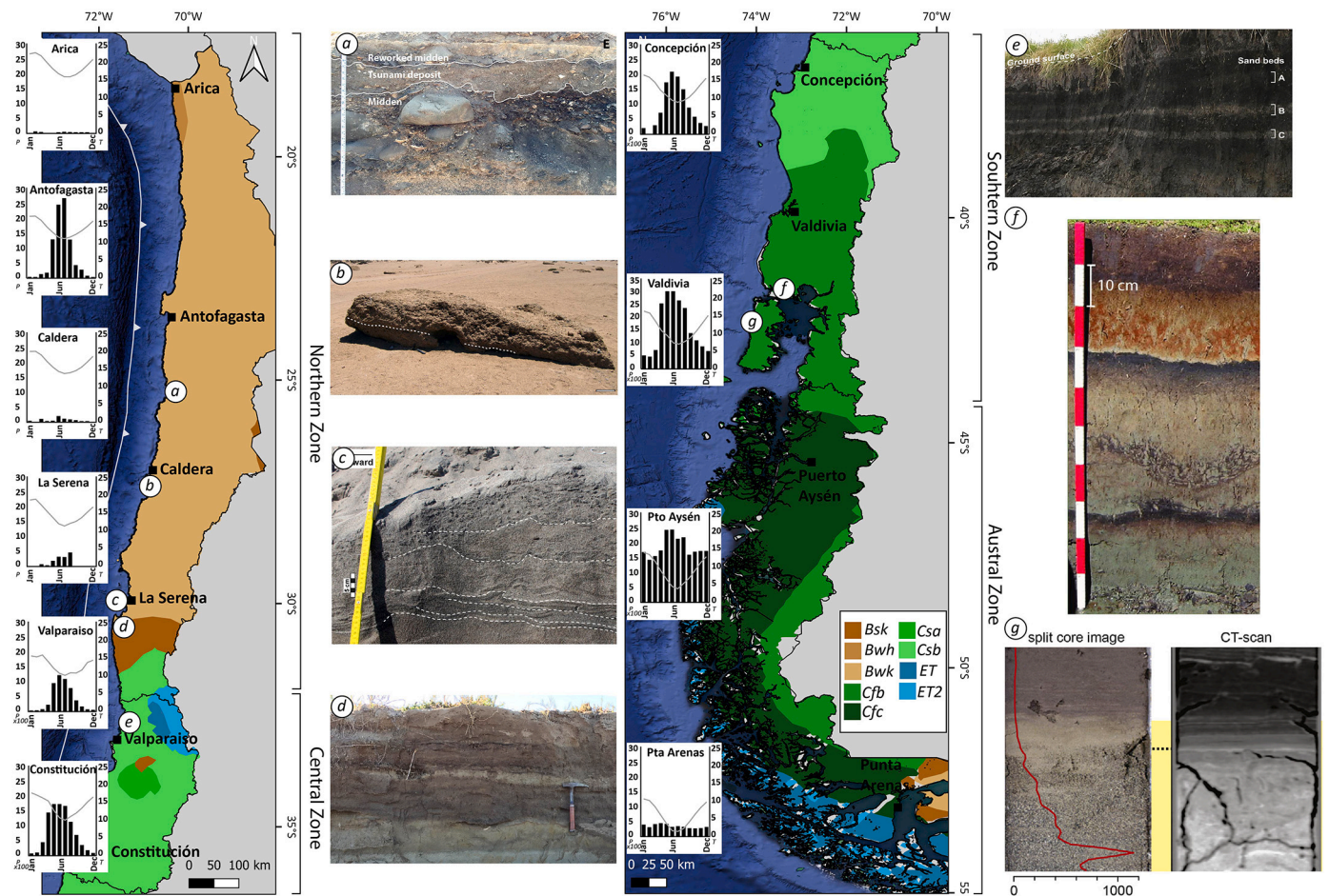


Fig. 2. Köppen-Geiger climate classification of Chile with examples of the tsunami deposits found in these coastal environments. Graphs show the average precipitation and temperature from 1978 and 2019 in the cities labelled on the map. a) A Holocene palaeotsunami found in archaeological sites (León et al., 2019). b) Boulders on an 18 m coastal cliff likely transported by the 1420 CE tsunami (Abad et al., 2020). c) Deposits of the 2015 tsunami at La Serena beach (Bahlburg et al., 2018). d) Tsunami and palaeotsunami deposit at Tongoy (Easton et al., 2022). e) Sandy evidence of Holocene subduction and tsunamis (Dura et al., 2015). f) Deposit of the 1960 tsunami and its predecessors (Cisternas et al., 2005). g) Palaeotsunami deposits in a sediment core and CT scan from a coastal lake (Kempf et al., 2017).

2.4. Criteria for assessing the confidence level of tsunami deposits

Since the interpretation of tsunami deposits is sometimes debatable (e.g., “is the deposit formed by a tsunami or is it an indicator of higher a sea-level?”), we created a system of criteria to assess the level of certainty of the tsunami interpretation for each deposit, following a similar methodology as shown in Lau et al., 2010. These criteria provide metric information about what has been done to identify the available information and thus establish where further analyses are needed, especially for those deposits where only a few criteria were met. It should be noted that this ranking is different to NOAA’s tsunami event validity scoring because we are specifically analysing the fundamentals to interpret tsunamis deposits and not the earthquakes that generate them. Each deposit presented in the literature was assessed against six criteria, defined as “Yes” or “No” questions. The six criteria (C1 to C5) and their rationales are:

C1. Does the tsunami interpretation include both physical (includes geological, chemical, biological and geomorphological) and cultural (include archaeological, anthropological e.g., oral history and written records, and contextual e.g., local knowledge of tsunamigenic source) evidence?

- The integration of both categories offers greater scope to interpret tsunami deposits. The description of each category is as defined by Goff et al. (2012b).

C2. Can this deposit be correlated with other deposits from the same/ other articles to suggest a tsunami origin?

- The wide spatial impact of tsunami waves should have created more than one deposit in the region; therefore a positive response increases the confidence level.

C3. Is there any historic counterpart or numerical model to validate the tsunami-origin at the deposit’s location?

- The existence of historical records or eyewitness accounts confirming the impact of tsunamis at that location can greatly increase the confidence level. Alternatively, numerical models used to simulate the inundation along the study area can also prove a deposit is associated with a tsunami.

C4. Have other mechanisms of marine inundation been considered in the original research?

- Confidence level increases if the authors of the article have discussed the differences and similarities between tsunamis and other marine inundation mechanisms that could impact the area, or/and have constructed rational arguments to confirm or reject a tsunami origin based on the evidence. Note that a “yes” response can be achieved even when other mechanisms cannot be ruled out, e.g., after

thorough discussions presented in the article, the authors concluded the deposit could have been created by a tsunami and/or storm waves.

C5. Is the deposit deemed a tsunami deposit with corroborating evidence?

- This can be achieved if the authors of the original research have done or assigned a critical evaluation of the deposit to propose its tsunami-origin, and there is no subsequent research to question or refute the tsunami interpretation.

The scoring system is out of five and the assignment of a “Yes” or “No” answer is described in [Table 1](#). The higher counts of “Yes” means the deposit is more likely a result of a tsunami.

3. Climatic macrozones and coastal setting along Chile

The coast of continental Chile (17°S to 56°S) is around 4200 km long, spanning several climatic zones. The main factors that control the climate in Chile are the Pacific Ocean, the Humboldt Current, the South Pacific High, and large morphotectonic elements such as the Principal Andes cordillera and Coastal range. We have adopted the climatic macrozones established by ([Ministerio de Obras Publicas, 2015](#)) that are, based on hydrographic, orographic, and climatic affinities. It is important to identify the type of climates characterized by these zones and we, therefore, use an updated version of the Köppen–Geiger climate classification based on long-term monthly precipitation and temperature station time series ([Peel et al., 2007](#)). [Fig. 2](#) shows four zones with their climate classification, alongside illustrations of the types of tsunami deposits recorded. The climatic characteristics of each macrozone are described in detail below.

3.1. Northern macro zone (18°S to 32°S)

This zone is characterized by a higher proportion of arid climate (B) on the coast and inland ([Fig. 2](#)). The northern part, from 18°S to 20°S, has a warm desert climate (BWh) with rare river outlets, with few cities like Arica and Antofagasta. Toward the south, the area is predominantly defined by a cold desert climate (BWk) on the coast and inland ([Fig. 2](#)). Both climates represent the main part of the Atacama Desert, considered to be the driest desert in the world ([Robinson et al., 2015](#)). Under these conditions, coastal landscapes comprise steep cliffs, uplifted rocky platforms and narrow plains. Additionally, the southern edge is characterized by a cold semiarid climate ([Fig. 2](#)) (BSk) where wetlands can be found. Along these coasts, precipitation might be scarce for years or even decades and only be intermittently disturbed by torrential downpours during bouts of moderate to intense El Niño Southern Oscillation (ENSO), which can cause debris flows and floods.

3.2. Central macro zone (32°S to 36°S)

This area has some of the largest cities in Chile such as Santiago, Valparaíso and Constitución, which support around 62% of the country's population. Here the weather conditions are humid with moderate rainfall (an average of 943 mm per year) concentrated in winter with a long dry season of 7–8 months ([Ministerio de Obras Publicas, 2015](#)). This zone is characterized by a temperate climate ([Fig. 2](#)) (C), more specifically by a warm summer mediterranean climate ([Fig. 2](#)) (Csb) with moderate precipitation, uniformly distributed from west to east. With high rainfall and frequent frost, this zone offers good conditions for the development of wetlands and estuarine systems close to river mouths. In this area, there are storms typical of rainy seasons that present different intensities of winds and can sometimes be very destructive with tidal waves on the coasts ([Campos-Caba and Beya, 2015](#)).

3.3. Southern macro zone (36°S to 44°S)

A temperate climate dominates this zone from the coast to the mountains, with two subdivisions. From ~36°S to ~39°S there is a warm summer mediterranean climate ([Fig. 2](#)) (Csb) with the remaining portion being more oceanic ([Fig. 2](#)) (Cfb). Precipitation is high, and there are abundant estuarine systems, lagoons, wetlands, and lakes at the coast. In addition, in this zone are the highest values of swells that have damaged coastal cities, according to historical records. ([Campos-Caba and Beya, 2015](#)).

3.4. Austral macro zone (44°S to 55°S)

Characterized by the presence of gulfs and fjords with a few cities like Puerto Aysén, this zone has the largest number of lakes and lagoons in Chile. This zone extends from ~66°W to ~76°W longitude, with the climate conditions varying from West to East. The western part, facing the coast, has a tundra climate ([Fig. 2](#)) (ET) while the eastern section toward the mainland has a subpolar climate ([Fig. 2](#)) (Cfc).

Overall, Chilean coastal climates vary from arid and hot conditions in the north to humid and cold toward the south. These conditions influence not only in the preservation of the deposit and consequently in their distribution, but also the type that may be found. These are discussed below.

4. Seismic studies and historic tsunamis in Chile

4.1. The history of seismic studies in Chile

The first records of earthquakes in Chile came from the 16th to 18th centuries, when Chile was part of the Spanish kingdom. For this reason, most of the documents that described historical tsunamis were Spanish administration letters reporting the aftermaths of the events ([Cisternas et al., 2012](#); [Stewart, 2019](#); [Udias et al., 2012](#)). One of the most relevant works of Chilean seismic history was done by Fernand de Montessus de Ballore, who analysed each earthquake between the arrival of Pedro de Valdivia in 1540 CE (The first Spanish conqueror) and the great Valparaíso earthquake of 1906 ([de Ballore, F. d. M., 1913](#)). This was a benchmark report for seismic studies in Chile and underpinned the methodologies for the forthcoming catalogues. This work was followed by [Lomnitz \(1970\)](#) who presented, for the first time, detailed information about the magnitude, location, and effect of early historical events (1535 CE–1955). Subsequent intensive work estimated the magnitude of large historical earthquakes based on tsunami run-up observations and vice versa (e.g., [Kausel, 1986](#); [Barrientos, 1980](#); [Ramírez, 1988](#); [Dorbath et al., 1990](#); [Kausel and Ramírez, 1992](#)). Additionally, other studies evaluated the spatial-temporal distribution of large earthquakes that occurred in some seismotectonic regions of Chile. For example, [Kausel \(1986\)](#) and [Comte and Pardo \(1991\)](#) proposed magnitudes and locations for several earthquakes in northern Chile that occurred prior to instrumental records, using isoseismal maps. Likewise, [Abe \(1979\)](#) applied a quantitative approach to evaluate the magnitude of tsunamigenic earthquakes in Chile since the end of the 19th century, analysing data from tide gauges deployed in the Pacific Ocean. These studies provide key information to help understand the seismicity of the country and underpinned future research.

In the following section, we detail all tsunamigenic earthquakes that have affected the coasts of Chile based on global databases, historical earthquake catalogues and written records reported in journal articles.

4.2. Historical tsunamis in Chile

Using the methods outlined in [section 2](#), we identified thirty-one historic tsunamigenic events in Chile. The first tsunami reports date to the XVI century event on the 8th of February 1570 CE in Penco ([Fig. 1](#)). The last megathrust event >Mw 8.0 included in this review is the 2015

Illapel tsunami. All thirty-one historical tsunamis were caused by earthquakes. Except for the 2007 Aysén earthquake (Mw 6.2), all tsunamigenic earthquakes were Mw 7.5 or higher. Figs. 3 and 4 show the spatial distribution of the epicentre of historical tsunamigenic earthquakes while Table 2 summarises the date, magnitude, and tsunami

reports of these events. Descriptions of each event are included in the supplementary information (Appendix A).

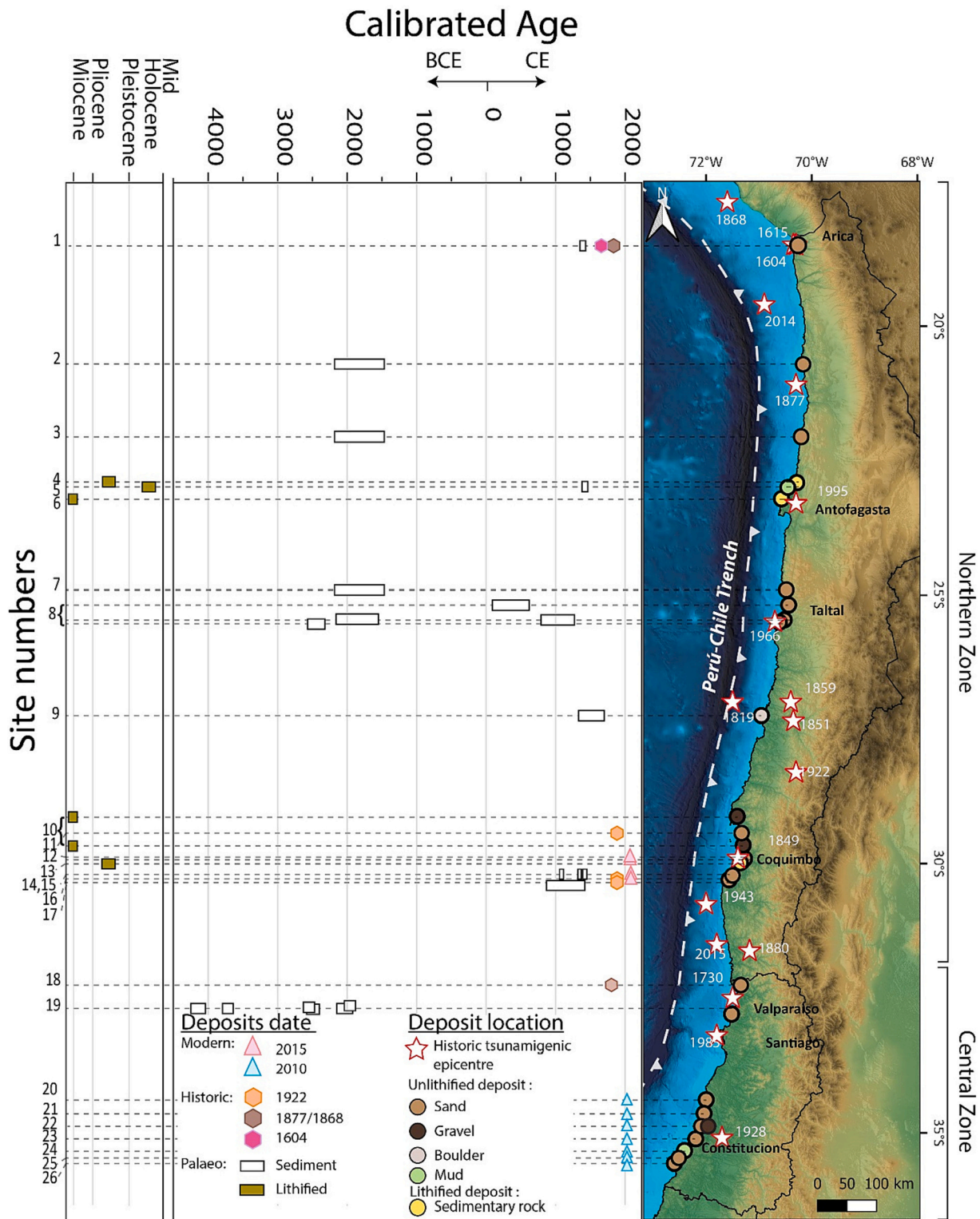


Fig. 3. Spatiotemporal compilation of tsunami evidence along the Northern and Central zone of Chile. Sites numbers are associated with Table 2 which describes the deposits and the validity of the evidence. Coloured triangles indicate evidence of valid historical events, brown and white rectangles show the age range of palaeotsunami deposits. Coloured circles indicate sediment grain size/lithified deposits. Red stars show the estimated epicentres of historical tsunamigenic events. (For interpretation of the references to colour in this figure legend, the reader is referred to the web version of this article.)

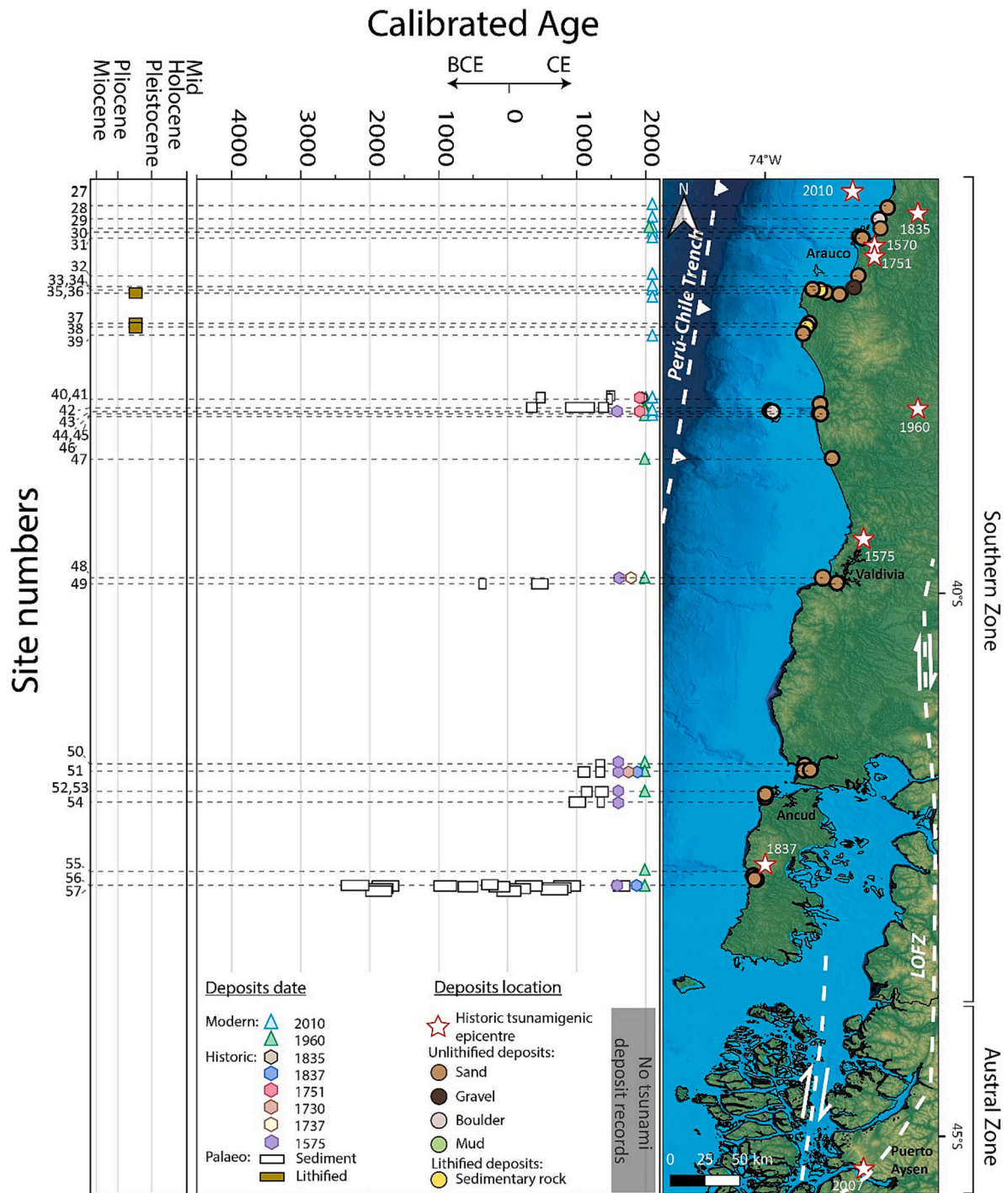


Fig. 4. Spatiotemporal compilation of representative tsunami evidence along the Southern and Austral zone of Chile. The sites number are linked with Table 2 which describes the deposit and the validity of the evidence. Coloured triangles indicate evidence of valid historical events, brown and white rectangles show the age range of palaeotsunami deposits. Coloured circles indicate sediment grain size/lithified deposits. Red stars show the estimated epicentres of historical tsunamigenic events. (For interpretation of the references to colour in this figure legend, the reader is referred to the web version of this article.)

5. Tsunami deposits in Chile

In Chile, tsunamis affect a wide range of coastal environments and can deposit sediments that range from muddy sand to boulders, which have been also interpreted in sedimentary rock. For this reason, we divided the evidence into lithified and unlithified records, and this last includes three categories according to the grain size. Among these, sandy deposits are the most common and reliable way to record the area flooded by tsunamis. However, their preservation and deposition have

always been confined to specific geomorphological settings, within low-lying and sheltered back-barrier settings (e.g., Szczuciński et al., 2005; Szczuciński et al., 2007; Szczuciński, 2012; Spiske et al., 2013a; Bahlburg and Spiske, 2015; Spiske et al., 2020). The environments that meet these conditions consist of lagoons, estuaries, coastal lakes, beach-ridge sequences, marshes, alluvial plains, and emerged sea caves (Engel et al., 2020). In continental Chile, the development of these geomorphological traps is limited to key sections of the coast associated with specific climate conditions.

Table 2
Historical tsunamigenic events in Chile. See Fig. 1 for locations.

Century	Date (CE)	Epicentre	Magnitude (Mw)	Tsunami reports (wave height, location)	Reference
16th	8th February 1570	Concepcion	8–8.8	2–4 m, Constitución*	Lomnitz (2004); SHOA, (2010); Stewart (2019)
	16th December 1575	Valdivia	8.5–9.5	4 m, Valdivia 1.5–2 m, Concepción*	CERESIS (1985a); Ruiz and Madariaga (2018)
17th	24th November 1604	Arica	8.7	20 m, Arica**	Comte and Pardo (1991); Fernandez (2007)
	16th September 1615	Arica	7.5	<1 m, Arica**	Comte and Pardo (1991)
18th	15th March 1657	Concepcion	8.8	4 m, Concepción*	Lomnitz (2004)
	8th July 1730	Valparaíso	9.0	10 m, Vina del mar 2 m, Japan	Soloviev (1984); Udias et al. (2012); Tsuji (2013); Carvajal et al. (2017a)
19th	24th May 1751	Concepción	8.5	3–5 m, Concepción**	Udias et al. (2012)
	11th April 1819	Caldera	8.5	2 m, Hawaii 4 m, Caldera 4 m, Constitución 3.6 m, Valparaíso	Abe (1979); Lomnitz (2004); SHOA (2010)
20th	20th November 1822	Valparaíso	8.5	12 m, Concepción	CERESIS (1985a); NOAA (2021)
	20th February 1835	Concepción	8–8.5	<1 m, Valparaíso	Lomnitz (2004)
	7th November 1837	Valdivia and Castro	8.0	8 m, Corral	Lomnitz (2004)
	17th November 1849	Coquimbo	7.5	5 m, Coquimbo	CERESIS (1985a, 1985b); Lomnitz (2004)
	26th May 1851	Huasco	7.5	3 m, Huasco	CERESIS (1985a, 1985b); Lomnitz (2004)
	5th October 1859	Copiapó	7.5	6 m, Caldera	CERESIS (1985a, 1985b); Lomnitz (2004)
	13th August 1868	Arica	8.8	25 m, Arica 6 m, Iquique 6 m, Mejillones 7.5 m, Coquimbo 7–8 m, New Zealand	Lockridge (1985); Comte and Pardo (1991); Lomnitz (2004); Okal (2010)
	10th May 1877	Iquique	8.0	10 m, Arica 3 m, Concepción 3.3 m, New Zealand	Monge and Mendoza (1993); Aránguiz et al. (2014); Borrero and Goring (2015); Ruiz and Madariaga (2018)
	15th August 1880	Illapel	7.5	<1 m, Coquimbo	Lomnitz (1970, 2004)
	17th August 1906	Valparaíso	8.4	2 m, Valparaíso 1.5 m, Penco and Tomé	CERESIS (1985a); NOAA (2021)
	4th December 1918	Diego de Almagro	7.8	5 m, Caldera	CERESIS (1985a); NOAA (2021);
	11th November 1922	Vallenar	8–8.5	9 m, Chañaral 1 m, Japan 1.5 m, Constitución	Abe (1979); Lomnitz (1970, 2004); Ruiz and Madariaga, (2018)
	1st December 1928	Talca and Constitución	8.4	<1 m, Los Vilos	Lomnitz (2004)
	6th April 1943	Illapel	8.3	0.9 m, Coquimbo and Tongoy	Lomnitz (2004)
	19th April 1955	Coquimbo	7.1	15 m, Ancud 10 m, Corral 10 m, Japan	CERESIS (1985a); NOAA (2021)
21st	22nd May 1960	Valdivia	9.5	10 m, Corral 10 m, Japan	Cisternas et al. (2005); Ruiz and Madariaga (2018)
	28th December 1966	Taltal	7.7	<1 m, Taltal	Deschamps (1980)
	3rd March 1985	Algarrobo	8.0	1.2 m, Valparaíso	Cisternas et al. (2005); Ruiz and Madariaga (2018))
	30th July 1995	Antofagasta	8.0	1.5 m, Antofagasta	Ruiz and Madariaga (2018)
	21st April 2007	Puerto Aysén	6.2	5–10 m, Puerto Chacabuco	Naranjo et al. (2009); NOAA (2021) CSN
	27th February 2010	Cobquecura	8.8	29 m, Constitución 12–15 m, Pichilemu	Fritz et al. (2011); Vargas et al. (2011)
	1st April 2014	Iquique	8.2	2 m, Arica, Pisagua Iquique	Ruiz and Madariaga (2018), NOAA (2021); CSN
	16th September 2015	Illapel	8.3	5–11 m, Coquimbo	Ruiz and Madariaga (2018)NOAA (2021); Easton et al. (2022);CSN

*Currently the city of Penco. ** At that time Arica was part of Perú and the Chilean border was at 24 S.

5.1. Temporal and spatial distribution of tsunami/palaeotsunami records

This review has found forty-eight publications that described tsunami evidence in fifty-seven sites throughout Chile and this section describes the distribution of modern, historical and palaeotsunami deposits located in onshore environments. For this review, modern tsunamis are those after the 1960 event when earthquakes and tsunamis started being well recorded through instrumentations.

5.1.1. Tsunami deposits from modern events

In Chile, most modern tsunami studies describe deposits related to three major events: The 9.5 Mw Valdivia in 1960, the 8.8 Mw Maule in 2010, and the 8.3 Mw Illapel in 2015.

The 1960 tsunami was a Pacific-wide event with the most significant deposits being laid down in southern Chile. For example, research in the Maullín estuary (Fig. 2f) reported a tsunami layer that matched with eyewitness reports of this event. Survivors indicated that most of the lower estuary was covered by a homogeneous layer of sand (Cisternas et al., 2000). In four trenches, a sandy layer (3–10 cm thick) at around 10 cm of depth was found between the pre-1960 muddy saltmarsh and modern soils. Grain size characteristics and the direction of the bent vegetation confirmed a landward transport of sand into the estuary. Therefore, based on sedimentological features and historical reports, researchers attributed this deposit to the 1960 tsunami (e.g., Cisternas et al., 2000). This is an example of how eyewitness accounts of tsunamis are important in providing context for when a tsunami occurred to support the interpretation of past event deposits, but such comments should be considered in conjunction with additional evidence to avoid ambiguity and subjectivity. Similarly, to identify the deposits of this and earlier events, (e.g., Cisternas et al., 2005; Brill and Cisternas, 2020) used buried soils and sand layers as an indicator of tectonic movement and tsunami flooding in an estuary halfway along the 1960 rupture.

Likewise, Atwater et al. (1992, 2013) investigated the development of erosion channels made by the 1960 tsunami as well as deposits of this and older tsunamis across a beach-ridge plain near Maullín. The studies supplied evidence of the 1575 CE tsunami and a past event dated between 1270 and 1400 CE, demonstrating the potential of using geomorphological changes together with deposits to identify tsunami inundation.

The 1960 tsunami also laid down deposits in the coastal lakes of southern Chile (e.g., Kempf et al., 2015, 2017, 2020). A study in lakes Cucao and Huelde (Fig. 2g) showed an abrupt emplacement of a 61 cm sandy layer with muddy rip-up clasts, in the seaward zone of these lakes. The deposits thinned inland to a thickness of 1.7 cm and interrupted the normal lake sedimentation that was, mainly characterized by organic-rich mud. Kempf et al. (2015) also used gravity cores together with sub-bottom and side-scan images to identify the horizontal and vertical distribution of tsunami signals across the lakes. Several studies in the Tirúa River floodplain have identified sandy deposits of the 1960 event intercalated with fine-grained floodplain sediments (e.g., Le Roux and Vargas, 2005; Ely et al., 2014; Nentwig et al., 2015; Bellanova et al., 2016; Nentwig et al., 2018), suggesting this floodplain is an important study area to understand tsunami and earthquakes recurrence. In additional, peat covered by a silt-sand layer and alterations associated with the co-seismic subsidence and tsunami in 1960 are documented in a coastal marsh in Chucalen and Mataquito (e.g., Garrett et al., 2013, 2015).

The earthquake of 27th February 2010 mainly affected southcentral Chile. Among the evidence for this event was, a variable coastal uplift of 240 ± 20 cm (Fig. 2e) and bleached coralline algae exposed after the mainshock (Vargas et al., 2011). Also, submerged quays, flooded beaches and river bars, flooded trees and swampy vegetation indicated subsidence of 50–100 cm at 110–120 km from the subduction interface, together with eroded vegetation, traces of beach erosion, and sand and boulder deposits associated to the tsunami impact on the coast. This study exemplifies how the identification of geomorphological changes and

sedimentary deposits are used in conjunction to analyse tsunami characteristics. Additionally, the 2010 tsunami's inflow at Isla Mocha entrained sands, gravels, and boulders that were found in the higher shoreface, on the beach, and along coastal terraces, showing the wide variation of the event's deposit. (Bahlburg and Spiske, 2012).

The 2010 tsunami backwash also caused significant erosion inland, scour around trees, and channel incision between 35°S and 37°S. According to an analysis of the backflow transport conditions of this mixed material, bedload transport was accomplished by supercritical flows, whereas deposition took place once currents on the low-gradient lower coastal plain had slowed down enough (Bahlburg and Spiske, 2012). In addition, boulders (≤ 1 m in diameter) were found transported up to 400 m inland (Morton et al., 2011). Similarly, three to five waves up to 10 m high deposited layers of sand and gravel over a wide range of environments including a coastal plain near a river mouth, river floodplains, coastal lagoons, a delta, alluvial valleys and a combined embayment and delta plain (e.g., Morton et al., 2011; Yoshii et al., 2012; Garrett et al., 2013; Chagué-Goff et al., 2015; Ely et al., 2014; Hong et al., 2016; Lario et al., 2016; Costa et al., 2019; Dura et al., 2017; Nentwig et al., 2018; Spiske et al., 2020) The thickness of these deposits did not exceed 80 cm and was mostly less than 30 cm (Lario et al., 2016).

Although the 2010 tsunami deposits reveal information about the processes that formed them, these data can be blurred by post-depositional taphonomic processes such as bioturbation and subaerial erosion, which alter the thickness, sedimentary structures, and grain size of the deposits (e.g., Bahlburg and Spiske, 2015; Spiske et al., 2020). Therefore, such changes need to be considered for subsequent numerical modellings where post-depositional processes can affect the reliability of these results. Overall, the 2010 tsunami is another example of where an understanding of the behaviour of tsunamis was achieved through the recognition of geomorphological changes and sedimentological features in the sedimentary sequence.

Most recently, the magnitude Mw 8.32015 Illapel earthquake generated a tsunami that affected northern Chile (Fig. 2c) (Ruiz and Madariaga, 2018). According to Bahlburg et al. (2018), this tsunami transported concrete boulders of up to two tonnes from the coastal road onto the beach and deposited a sandy laminated package of variable thickness on the beaches of Coquimbo and La Serena. Sedimentary structures such as cross-beds, sand diapirs and sand volcanoes were also identified. The study demonstrated that assemblages of sedimentary structures indicate a rapid deposition from one or several waves associated with the tsunami at these sites.

Another study of the 2015 tsunami recorded runups and inundation heights measured along 700 km of coastline from Chañaral to Concón (Aránguiz et al., 2015). The study indicated a maximum runup of 10.8 m in one small bay, suggesting that in general, runups rarely exceed 6 m. In contrast, Easton et al. (2022) show systematic run-ups to 10–11 m along the southwestern coast of Punta Lengua de Vaca. The results of a numerical model indicated that this difference is associated with a complex patched rupture of the causative earthquake, which started nearest to the coast and then propagated toward the trench involving the lower continental slope as well as the local bathymetry and topography. DePaolis et al. (2021) revealed sandy deposits related to the 2015 event at Pachingo marsh in Tongoy Bay in north-central Chile. Sandy layers were found between silty organic deposits and a tsunami interpretation was supported by historic evidence, geochemical analyses, geochronology, and stratigraphic studies. Other research measured run-up heights and coseismic movements along the affected area from Punta Teatinos and Los Vilos (Easton et al., 2022). In the same study, sandy deposits recorded the inundation of this event at Coquimbo-La Serena embayment, Tongoy, and Limarí river mouth areas, in addition to distinctive sandy layers interpreted as palaeotsunamis in the Tongoy riverine system. Unlike the 1960 and 2010 tsunamis, there are few sedimentological studies of this tsunami largely because the aridity of the coastal landscapes hamper tsunami deposit recognition.

Modern tsunamis like these can provide unequivocal evidence

Table 3

Compilation of site locations throughout Chile where Modern (Mode), Historic (Histo) and prehistoric (Palaeo) tsunami deposits have been recorded. The criteria fulfillment count is out of six points and the individual achievement for each layer is specified the Supplementary B material. Specific map locations are shown in Figs. 3 and 4. Proxy data used: Geo-Geological, Geom-Geomorphological, Chron-Chronological, Bio-Biological, Chem-chemical, Arch-Archaeological, Antr-Anthropological and Con-Contextual.

Site (#)	Site name /Macrozone	Number of events	Modern (Mode), Historic (Hist) and/or prehistorical (Palaeo) event	Physical Criteria	Environment	Proxy data	Inferred date	Criteria fulfillment count	Article
1	Arica /North	3	Histo and Palaeo	Two layers of medium to coarse sandy layers with sharp basal contact, erosive channels, cross bedding, archaeological artifacts, and rip-up clasts; between alluvial and wetland deposits	Coastal plain	Geo, Geom, Chron, Bio, Chem, Con	1720–1952 CE 1343–1891 CE 771–991 CE 370–772 CE	4 4 2 2	Muñoz Cupitty (2019), unpublished results
2, 3, 7	Pabellón de Pica, Paquica, Zapatero /North	1	Palaeo	Distinctive layers in midden with basal erosional contact, landward imbrication, high frequency of marine microorganisms (echinoderm spikes and red algae), reworked marine and archaeological material	Coastal plain	Geo, Geom, Chron, Bio, Chem, Arch, Con	3481–3448 BP 5033–5270 BP 3969 BP	4 3 3	Salazar et al. (2022)
4	Hornitos /North	1	Palaeo	Conglomerate bed of angular boulders set in a matrix of very poorly sorted fine to very coarse-grained shell-rich sandstone with erosional basal contact.	Shoreface cliff	Geo	Plio-Pleistocene	1	Hartley et al. (2001)
5	Mejillones bay /North	3	Palaeo	Sediment destabilisation was recorded by an angular unconformity, lenticular coarse deposit and slumping in shallow marine core.	Shallow marine platform	Geo, Geom, Chron, Bio, Chem.	1408–1449 CE 1754–1789 CE Mid-Late Holocene	3 3 1	Vargas et al. (2005)
6	Caleta Herradura /North	1	Palaeo	Two chaotic and poorly sorted breccia units present an erosive base with inverse to normal grading.	Shoreface cliff	Geo	Miocene	1	Cantalamessa and Di Celma (2005)
4	Hornitos /North	1	Palaeo	Downward sandstone dyke injection by tsunami mass backflow failure in breccia outcrops.	Shoreface cliff	Geo	Possibly Messinian	1	Le Roux (2015)
8	Taltal /North	3	Palaeo	Sandy layers cutting archaeological occupation layers-likely responsible for notable occupation changes.	Coastal plain	Geo, Geom, Chron, Bio, Chem, Con	4491 ± 27 cal BP 1498 ± 217–1087 ± 199 BP 3990 ± 286 BP 1761 ± 238 BP	4 2 4 2	León et al. (2019)
9	Cisnes' bay /North	1	Palaeo	Cliff-top (>18.5 m a.s. l.) boulder deposit above the limit of modern storm waves and > 284 m inland	Coastal plain	Geo, Geom, Chron, Con	1288–1635 CE (1420)	4	Abad et al. (2020)
4, 5, 10, 29, 39	Mauullín, Mejillones, Hornitos, Carrizalillo, Ranquil, Caldera, Los Hornos /South and North	6	Histo and Palaeo	Tsunami deposits form Miocene to modern times. Typical flooding features are: Well-rounded mega clast from beaches, sand injections, basal shear carpets and megaflutes at the base of scoured channels.	Coastal plain and shallow marine platform	Geo, Geom, Chron.	1960 CE 1408–1449 CE 1754–1789 CE Mid-Late Holocene, – Plio-Pleistocene, – Plio-Pleistocene, – Miocene-	5 4 2 1 1 1 1	Le Roux and Vargas (2005)
11,18	Quebrada Teatinos,	2	Histo	Sand units, indicated by an erosive contact to an	Coastal plain		1714–1955 CE (1922)- 1697–1950 CE (1730)-	3 3	May et al., 2013

(continued on next page)

Table 3 (continued)

Site (#)	Site name /Macrozone	Number of events	Modern (Mode), Historic (Hist) and/or prehistorical (Palaeo) event	Physical Criteria	Environment	Proxy data	Inferred date	Criteria fulfillment count	Article
	Pichicuy bay/ North			underlying mud, mud clasts, and basal gravel components. Also, thin sand sheets in a coastal swamp deposit but marine faunal elements, or typical sediment structures such as fining-up sequences or erosive contacts were not detected.		Geo, Geom, Bio			
12	Playa Changa and La Serena /North	1	Mode	Parts of the coastal road embankments and boulders deposited landward. Laminated lenticular package of light-coloured sand layer rich in heavy minerals.	Coastal plain	Geo, Antr, Con	2015 CE 2015 CE	5 5	Bahlburg et al. (2018)
13	Herradura bay /North	1	Palaeo	Scattered large boulders embedded in a Pleistocene shelly marine terrace (30–40 m a.s.l.)	Coastal plain	Geo, Chron.	Middle Pleistocene	1	Paskoff, 1991
14	Tongoy /North	4	Mode and Palaeo	Fine sandy layers with irregular basal contacts, laminations, rip-up clasts, benthic foraminifera interbedded between alluvial fine sediments.	Tidal Marsh	Geo, Geom, Chron, Bio, Chem	2015 CE 1108 ± 77 CE 1346 ± 77 CE 1473 ± 77 CE-	5 2 2 4	Easton et al. (2022)
15	Tongoy /North	1	Mode	Sediment mark on Tongoy town left by tsunami waves.	Coastal plain	Geo, Antr	2015 CE	4	Contreras et al. (2016)
16	Pachingo marsh /North	2	Mode and Histo	Two tabular sand sheets. Both deposits are composed of poorly to moderately sorted, grey-brown, fine-to-medium-grained sand and are distinct from underlying and overlying organic-rich silt. Both sand beds thin (from ~20 cm to <1 cm) and fine landward and show normal grading.	Tidal Marsh	Geo, Chem, Chron, Antr	2015 CE 1862–1952 CE (1922)	5 5	DePaolis et al. (2021)
17	Pachingo marsh /North	2	Histo and Palaeo	Layer of coarser grain size, high content of seashells, greater amounts of gravel and the presence two rip-up clasts.	Tidal marsh	Geo, Chron, Bio, Chem	1918 ± 26 CE (1922) 858–1468 CE (1420)	4 4	Araya et al. (2022)
19	Quintero /Central	6	Palaeo	Lateral extensive sand layers with sediment properties and diatoms assemblages that point to a tsunami source.	Tidal marsh	Geo, Chron, Bio, Con	3830–4085 BP 3711–3974 BP 4242–4519 BP 4857–5259 BP 5492–5732 BP 5931–6182 BP	2 2 2 2 2 2	Dura et al. (2015)
20	Petrel lagoon /Central	1	Mode	A layer of medium to fine sand containing rock clasts, overlain by a thin, silty, fine sand layer. Ostracods and diatoms were abundant and small number of benthic and planktonic foraminifera.	Lagoon	Geo, Bio, Con	2010 CE	2	Horton et al. (2011)
21		1	Mode				2010 CE	5	

(continued on next page)

Table 3 (continued)

Site (#)	Site name /Macrozone	Number of events	Modern (Mode), Historic (Hist) and/or prehistorical (Palaeo) event	Physical Criteria	Environment	Proxy data	Inferred date	Criteria fulfillment count	Article
	Bucalemu /Central			Cobbles and boulders transport 155 m inland. Sand covering plants and fine-grained cap on the top of tsunami deposit. Scours structures.	Coastal plain and River floodplain	Geo, Antr, Con	2010 CE	5	Spiske and Bahlburg (2011)
22, 34	Mataquito, Arauco/ South	1	Mode	Geomorphological context to study controlling factor in the intensity of mechanical imprints on the surface of quartz grains transported by tsunamis and deposited in the inner shelf and coastal areas	Coastal plain	Geom, Geo, Antr	2010 CE 2010 CE 2010 CE 2010 CE	4 4 4 4	Costa et al. (2019)
23, 24, 27, 28, 32	La Trinchera, Constitución, Purema, Coliumo, Talcahuano /Central and South	1	Mode	Scour and planation of the land surface, inundation scour around the bases of trees, and channel incision from return flow. Sheets of sand/ gravel and boulders were transported 400 m inland.	Coastal plain	Geom, Geo, Antr, Con	2010 CE 2010 CE 2010 CE 2010 CE 2010 CE	45 5 5 5 5	Morton et al. (2011)
23	La Trinchera,	1	Mode	Sediments consisting of cobbles and sand had a maximum thickness of 20 cm, massive sand deposits were up to 15 cm thick.	Coastal plain	Geom, Geo, Antr, Con	2010 CE	5	Spiske et al., 2020
25	Las Cañas /Central	1	Mode	Sandy's deposit was laid down between 160 and 260 m inland. It consisted of a medium to coarse sand that thinned and fined inland. Geochemical analyses and diatom assemblages confirm a marine origin.	Coastal plain	Geom, Geo, Bio, Antr, Con	2010 CE	5	Chagué-Goff et al. (2015)
26, 30, 39	Loanco, Chome, Lebu, /South	1	Mode	Coseismic coastal change was measured using geomorphologic and anthropogenic markers. Pervasive marks in vegetation, traces of erosion on beach, sand, and boulder deposits.	Coastal plain and cliff	Geo, Geom, Bio, Con	2010 CE 2010 CE 2010 CE	5 5 5	Vargas et al. (2011)
29, 45, 53	Rio Andalien, Tirúa River, Chucalen/ South	1	Mode	The 1960 and 2010 tsunami deposits are fragmentary, variable and have no unique, diagnostic diatom assemblage	Coastal plain	Geo, Chro, Bio, Con	2010 CE 2010 CE 1960 CE 2010 CE 1960 CE 1960 CE	4 4 4 4 4 4	Garrett et al. (2013)
31, 32, 33, 36	Talcahuano, Playa Blanca, Arauco and Llico /South	1	Mode	Soils and tsunami deposits are rich in water-soluble ions (Na ⁺ , Mg ²⁺ , Cl ⁻ , Br ⁻ and SO ₄ ²⁻)	Coastal plain	Geo, Antr, Chem, Con	2010 CE 2010 CE 2010 CE 2010 CE	5 5 5 5	Yoshii et al. (2012)
28	Llico and Tubul /South	1	Mode	Coseismic deformation measured by Lithotamiun algae and <i>Mytilus chilensis</i> . A centimetre-scale fine sandy layer, with crustaceans and some fish, flooded 650 m	Coastal plain	Geom, Geo, Bio, Con	2010 CE 2010 CE	5 5	Lario et al. (2016)

(continued on next page)

Table 3 (continued)

Site (#)	Site name /Macrozone	Number of events	Modern (Mode), Historic (Hist) and/or prehistorical (Palaeo) event	Physical Criteria	Environment	Proxy data	Inferred date	Criteria fulfillment count	Article
35, 37, 38	Caleta La Poza, Punta Huenteguapi and El Cuco /South	1	Palaeo	inland. Houses and cars sweep out to sea. Sandstone dykes and sills were injected from the tsunami backwash. Tsunami-bearing sedimentary structures such as rip-up intraclast, inverse gradation, planar laminae, ripple, and trough cross-lamination.	Coastal plain	Geo, Bio.	Possibly Pliocene Possibly Pliocene Possibly Pliocene	2 2 2	Le Roux et al. (2008)
40	Quidíco /South	5	Mode, Histo and Palaeo	Five tabular sand beds are laterally extensive, well-sorted, fining upward, have sharp lower contacts, and contain brackish and marine diatom assemblage extending as much as 1.2 km inland. Eyewitness accounts of tsunami inundation	River floodplain	Geo, Geom, Chron, Bio, Con	2010 CE 1960 CE 1820-1960 CE (1835) 1690-1910 CE (1730 or 1751)- 1445-1490 CE 1450-1430-1610- 1615 CE	5 5 4 4 2 2	Hong et al. (2016)
41	Tirúa and Quidíco /South	3	Palaeo	Stratigraphic, lithological, and diatom results show variable coseismic land-level change coincident with tsunami inundation	River floodplain	Geo, Chron, Bio, Con	2010 CE 1960 CE 1835 CE 1640-1800 CE (1751) 1500-1630 CE (1575) 1520 + -50 CE 1440 + -15 CE 340 + -70 CE	4 4 4 4 4 2 2 2	Dura et al. (2017)
42	Tirúa river /South	5	Mode, Histo and Palaeo	Six distinct, successive tsunamigenic sand layers intercalated in fine-grained floodplain sediments. OSL dating revealed a heterogeneous equivalent dose distribution with increased over-dispersion values in the upper parts of the profile.	River floodplain	Geo, Chron, Con	1940 ± 10 CE (1960) 1730 ± 100 CE (1730-1751) 1310-1470 CE 830-1250 CE 490-530 CE	4 5 2 2 2	Nentwig et al. (2015)
42	Tirúa river /South	5	Mode, Histo and Palaeo	Sand layers are characterized by erosional bases and landward thinning and fining, consisting of well-sorted, unimodal sand and diatom data also indicate environmental changes caused by neotectonic movement. Six different events are connected to vertical neotectonic movements that occurred at the central Chilean margin during the last 1500 yr.			2010 CE 1940 ± 10 CE (1960) 1730 ± 100 CE (1730-1751)- 1300-1500 CE- 850-1250 CE- 400-600 CE-	4 4 4 2 2 2	Nentwig et al. (2018)
43	Isla Mocha /South	1	Mode	Tsunami inflow entrained sands, gravels, and boulders up to 600 m and 300 m inland respectively. Widespread progradation and imbricated fans of	Coastal plain	Geo, Geom, Con	2010 CE 2010 CE	5 5	Bahlburg and Spiske (2012)

(continued on next page)

Table 3 (continued)

Site (#)	Site name /Macrozone	Number of events	Modern (Mode), Historic (Hist) and/or prehistorical (Palaeo) event	Physical Criteria	Environment	Proxy data	Inferred date	Criteria fulfillment count	Article
43	Isla Mocha /South	1	Mode	coarse sediments developed downstream of terrace steps during backflow.	Coastal plain	Geo, Geom, Con	2010 CE	5	Bahlburg and Spiske (2015)
44	Tirúa /South	4	Mode and Histo	Tsunami onshore deposits modified by early diagenesis. Sand layers 2 km upriver interbedded with silty floodplain sediments characterized by well-sorted, rounded, medium-grain size and sharp lower contact.	River floodplain	Geo, Geom, Chron, Bio, Antr, Con	2010 CE 1960 CE 1640–1800 CE (1751) 1500–1630 CE (1575)	5 5 4 4	Ely et al. (2014)
46	Tirúa /South	2	Mode	Grey sand deposits yield sharp erosional base contacts, few rip-up clasts and thinning inland.	Estuary	Geo, Antr, Con	1960 CE 2010 CE	5 5	Bellanova et al. (2016)
47	Imperial /South	1	Mode	Massive clear sandy sediments show lower erosive contact and no structure.	Tidal marsh	Geo, Chron, Con	1960 CE	5	Barra et al. (2004)
48	Chaihuín /South	3	Mode, Histo and Palaeo	Sand layers with sharp lower contacts and transitional upper contacts, upward and landward fining and marine diatoms.	Tidal marsh	Geo, Chron, Bio, Con	1960 CE 1600–1820 CE (1737) 1486–1616 CE (1575)	4 4 4	Hocking et al. (2021)
49	Las Coloradas /South	2	Palaeo	Marsh and meadow soils are abruptly overlain by sandy layers. Diatom's assemblages unclear	Estuarine	Geo, Chron, Bio	1700–1300 BP 2700–1700 BP	2 1	Nelson et al. (2009)
50	Caulle /South	4	Mode, Histo and Palaeo		Coastal plain	Geo, Geom, Chron, Antr	1960 CE Unknown - Unknown - Unknown -	4 1 1 1	Atwater et al. (1992)
50	Caulle /South	3	Mode, Histo and Palaeo	Eyewitnesses of flooding and fan deposits identify the levels that tsunamis and pre-events have reached.	Coastal plain	Geo, Geom, Chron, Antr, Con	1960 CE 1450–1620 CE (1575) 1270–1400 CE	5 4 2	Atwater et al. (2013)
50	Chuyaquen /South	3	Mode, Histo and Palaeo	Continuous tabular sand sheets alternated with darker organic marsh soils, giving the stratigraphy a horizontally banded appearance.	Tidal marsh	Geo, Chron, Con	1960 CE 1450–1610 CE (1575) 1020–1180 CE	4 4 2	Brill and Cisternas (2020)
51	Maullín /South	1	Mode	An eyewitness reported sand deposition in rivers and marshes. The layer has a sharp contact and buries vegetation.	Estuary	Geo, Con	1960 CE	4	Cisternas et al. (2000)
51	Maullín /South	5	Mode, Histo and Palaeo	Soil deposits buried by sand layers traced more than 1 km inland that resembles a modern tsunami deposit, record tectonic subsidence and tsunami inundation.	River floodplain	Geo, Chron, Bio, Con	1960 CE 1450–1510 1590–1620 CE CE CE (1575)- 1280–1390 CE 1021–1181 CE 84–330 CE	5 5 2 1 1	Cisternas et al. (2005)
52	Chucalen /South	4	Mode, Histo and Palaeo	Laterally extensive sand sheets traced 80 m thinning inland, contain marine or brackish diatom assemblages,	Tidal marsh	Geo, Chron, Bio, Con	1955–1971 CE (1960) 1540–1800 CE (1575) 1270–1450 CE 1070–1220 CE	5 5 3 2	Garrett et al. (2015)

(continued on next page)

Table 3 (continued)

Site (#)	Site name /Macrozone	Number of events	Modern (Mode), Historic (Hist) and/or prehistorical (Palaeo) event	Physical Criteria	Environment	Proxy data	Inferred date	Criteria fulfillment count	Article
54	Cocotue /South	4	Mode, Histo and Palaeo	suggesting tsunami deposition Soil horizons are buried locally by sand sheets like the modern beach with freshwater diatoms assemblages and sharp lower contact.	Coastal plain	Geo, Chron, Bio, Antr, Con	1960 CE 1505–1949 CE (1837) 1412–1625 CE (1575) 1505–1802 CE 1305–1435 CE 1300–1398 CE 898–1398 CE 898–1128 CE	5 4 5 2 2 3 2 3	Cisternas et al. (2017)
55	Cucao and Huelde lakes /South	1	Mode	Facies of mud rip-up clasts in a sandy matrix, medium to fine massive sand, organic-rich silt and sand, and mud cap with erosional contact in lake core sediments.	Coastal lake	Geom, Geo, Chron, Antr, Con	1960 CE	5	Kempf et al. (2015)
56	Cucao Lake /South	16	Mode, Histo and Palaeo	Lateral extended sandy clastic layers interbedded with lake deposits identified in core sediments and acoustics reflectors.	Coastal lake	Geom, Geo, Chron, Antr, Con	–11–5 BP (1960) 185–418 BP (1575) 894–1274 BP 1031–1418 BP 1079–1466 BP 1454–1832 BP 1624–1986 BP 1765–2109 BP 1914–2213 BP 2077–2322 BP 2378–2662 BP 2670–3001 BP 3530–3906 BP 3612–3994 BP 3626–4011 BP 3959–4344 BP	5 5 2 2 2 3 2 2 1 3 3 3 1 3 3 1 1 1	Kempf et al. (2020)
57	Huelde lake /South	17	Mode, Histo and Palaeo	Sandy layers with mud rip-up clasts, massive sand, and a mud cap in the lake. Layers share sedimentary similarities with the deposit of the 1960 CE tsunami.	Coastal lake	Geom, Geo, Chron, Con	–12 BP (1960) 101 BP (1837) 303 BP (1575) 553–970 BP 655–764 BP 1185–1185 BP 1604–1786 BP 1761–1926 BP 1903–2006 BP 2302–2302 BP 2821–2821 BP 3407–3407 BP 3897–3897 BP 4011–4011 BP 4535–4535 BP 4603–4603 BP 5360–5360 BP	5 5 4 2 3 2 3 1 2 2 2 1 2 1 1 1 2	Kempf et al. (2017)

regarding the attributes of the waves, characteristics of their deposits, and other criteria used to interpret the behaviours of older tsunamis from the stratigraphic record. Field observations of flow depths, flow directions, and inundation distances from modern tsunamis are also critical for constraining numerical models of inundation and sediment transport to conduct hazard assessments for populated areas (e.g., Morton et al., 2011).

Therefore, geological deposits of modern tsunamis from the 1960, 2010 and 2015 events are well constrained by instrumental and eyewitness reports that support the interpretations.

5.1.2. Historical tsunamis and palaeotsunami deposits

Despite the high frequency of tsunamis, there is little geologic

evidence of pre-1960 historical tsunamis in Chile. According to this review, thirty-one historic tsunamigenic events (Table 2) have been reported in Chile but only twelve have had some form of geological evidence identified (Table 3). These include a study from Arica (site #1 in Fig. 3) that recorded two sandy layers with tsunami features such as cross and convoluted bedding, erosive contacts with their underlying beds, rip-up clasts, moderate to poorly sorted matrices with gravel-sized clasts, fossil evidence and anthropogenic debris (Muñoz Cupitty, 2019). The first layer most likely corresponds to the 1868 CE or 1877 CE event and the second to 1604 CE tsunamis. Two works at Panchingo marsh (site #16 and #17 in Fig. 3) recorded a sandy layer deposited between organic-rich silt. It has tsunami features with similar characteristics to deposits from the 2015 event and dating results indicate that were most

likely laid down by the 1922 CE event in Vallenar (e.g., DePaolis et al., 2021; Araya et al., 2022). Likewise, in the Quidico riverbank (site #40 in Fig. 4), two tsunami layers dated using ^{137}Cs and ^{14}C match with historical accounts of the 1835 CE and 1751 CE events (Hong et al., 2016). Researchers also found historical tsunami layers accompanied by land elevation changes in the Tirúa estuary (site #42, #44 and #52 in Fig. 4) (e.g., Ely et al., 2014; Garrett et al., 2015; Nentwig et al., 2015; Nentwig et al., 2018). The upper layers represent the 2010 and 1960 events, while the others are likely associated with the 1751 and 1575 CE tsunamis from central Chile. It should be noted that tsunami deposits linked with the 1575 event have also been identified in several environments (marsh, river terrace, estuary, coastal plain and coastal lakes) of southern Chile (e.g., Cisternas et al., 2000; Cisternas et al., 2005; Garrett et al., 2015; Kempf et al., 2015; Cisternas et al., 2017; Kempf et al., 2017; Brill and Cisternas, 2020; Kempf et al., 2020). In addition, a study in Chaihuín (site #48 in Fig. 4) observed sandy layers with sharp lower contacts, transitional upper contacts and marine diatoms that come finer upward and landward (Hocking et al., 2021). The youngest layer was associated with the 1960 event and the oldest to the 1575 CE tsunami. A layer in between these two was linked to an event in 1737 CE of which there is a limited historic report. Finally, scarce evidence of the events of 1730 CE, 1835 CE and 1837 CE have been recorded in southern Chilean sites (e.g., Cisternas et al., 2005; Hong et al., 2016; Kempf et al., 2017).

Prior to the historical records, geological evidence for palaeotsunami has been identified at 92 deposits along the Chilean coast. The next section summarises and identifies common tsunami signatures from each macrozone.

5.1.2.1. Deposits in the northern macrozone. Fifteen sites described palaeotsunami records along the arid coast of northern Chile (Fig. 3). In Arica, two tsunamis were identified between wetland deposits at an archaeological site (site #1). The layers become thinner inland, contain rip-up clasts and according to radiocarbon analyses the deposits correspond to events that occurred between 771 and 991 CE and 370–772 CE (Muñoz Cupitty, 2019, unpublished results). Likewise, recent work has described palaeotsunami evidence in three archaeological sites along 1000 km of the northern coast (sites # 2–3 and 7) that disrupted the behaviour of prehistoric communities around 3800 BP (Salazar et al., 2022). The evidence shows layers of sand deposits with reworked marine material and erosional surfaces both overlying archaeological strata as well causing landward imbrication of shells and pebbles. According to the authors, the tsunami was most likely triggered by a \sim Mw9.5 earthquake along the major northern Chile seismic gap offshore of Taltal. Further south in Bahía Cisnes (site #9), a study identified a boulder field with clasts weighing up to forty tonnes. This is located 280 m inland from the coast and lies on top of an 18.5 m cliff (Abad et al., 2020). Radiocarbon analyses of well-preserved mollusc samples from below the boulders indicate a date of deposition between 1288 CE and 1693 CE. It should be noted that the arrangement of these boulders is scattered and isolated as opposed to ridge-like and is embedded in a sandy horizon beyond the limits of modern storm waves. A correlation between tsunami records from northern Chile, Hawaii, Henderson Island and Japan indicates that these boulders could be attributed to a tsunami that affected the Ibaraki Prefecture of Japan on 1 September 1420 CE (e.g., Tsuji, 2013; Namegaya and Yata, 2014). There is no definitive source at present for this event although evidence suggests that it might have originated in northern Chile (e.g., Nichol et al., 2003; Tsuji, 2013). Research in the shallow marine basin of Mejillones Bay (site #5) identified a major slump dated between 1409 and 1499 CE (Vargas et al., 2005), that may be associated with this event. In addition, at Tongoy riverine system (site # 14), a distinctive layer of sand with an erosional basal contact and, marine foraminifera content that thins landward, was constrained at 1473 ± 37 CE likely related to this same event (Easton et al., 2022). Moreover, the study observed others sandy deposits dated 1108 ± 77 CE and 1346 ± 50 CE that resemble the 2015 tsunami

identified in the area.

At Taltal (Fig. 3 site #8), León et al. (2019) identified two sand layers containing reworked archaeological material that have numerous characteristics indicative of tsunami deposition. These features include basal erosional contacts, flame structures, inverse grading, a mix of well-rounded and subangular gravels embedded in a sandy and fine matrix, and high concentrations of rocky intertidal shellfish species. Radiocarbon dates from shells and charcoal suggest that these layers were deposited by large Holocene palaeotsunamis dated close to \sim 4000 and \sim 1087 cal. Years BP. The authors considered Holocene sea-level variations and local uplift rate to conclude that run-ups (11 m) from these palaeotsunamis were greater than those (7 m) reported for historical reports in the area.

Earlier palaeotsunami events have been reported in lithified sediments in this zone. For example, two studies reported an array of tsunami signatures in rock sections in Mejillones (sites # 6 and 4), such as unusually coarse grain size in comparison to the surrounding deposits, erosional bases, mixed sediment source, normal grading or massive texture at various coastal sections in northern Chile (e.g., Cantalamezza and Di Celma, 2005; Le Roux and Vargas, 2005). Cantalamezza and Di Celma (2005) indicated that Miocene sandstones were deposited by a density flow during a tsunami backwash, due to marked facies changes from low to high energy shoreface environments. Similarly, Le Roux and Vargas (2005) found tsunami backwash signatures associated with a possible Plio-Pleistocene event in Hornitos (site #10) due to the presence of scouring and the incorporation of mixed sediment sources within the proposed tsunami deposit. The inferences from both studies are further corroborated by the active tectonic regime of this area since the early Miocene and by the marked seaward shift of the facies that overlie the purported tsunami layers, which is thought to be related to a coseismic uplift of the sea floor. It should be noted that some authors have argued that these deposits could be evidence of a palaeomegatunami triggered by the impact of Asteroid Eltanin in the South Pacific around 2.51 ± 0.07 Ma (Goff et al., 2012a).

These studies discussed above indicate that palaeotsunami deposits can be found in northern Chile despite the arid and geomorphological conditions (rocky, narrow, and steep coastal plains) that tend to hamper the preservation of recent events. It is plausible that only deposits related to exceptionally large events can survive in such extreme climatic conditions.

5.1.2.2. Deposits in the central macrozone. There are numerous records of the 2010 tsunami preserved here, but palaeotsunami deposits are scarce (Fig. 3). Only in site #19 palaeotsunami evidence has been reported by tracing six laterally continuous sand beds in Quintero's lowland (Dura et al., 2015). Dated plant remains from the bottom of sand beds revealed that these layers were deposited around 6200, 5600, 5000, 4400, 3800, and 3700 calibrated yr. BP. The sediment properties and diatom assemblages of the layers showed anomalous marine planktonic diatoms and upward fining of silts, both pointing to a marine sediment source and high-energy deposition. Indeed, this kind of lowland environment is ideal for protecting and trapping tsunami deposits. Their high sedimentation rate allows for better preservation and exhibits clearer contrast between light-coloured tsunami sands and darker organic soils, leading to the easy identification of tsunami layers. This will be discussed further in Section 5.

It should be noted that in this macrozone, despite the recognized frequency of tsunamis in historical times, the record is scarce, which may be influenced by the important levels of urbanization that do not lead to the preservation of palaeotsunami deposits and/or that little has been explored.

5.1.2.3. Deposits in the southern macrozone. In this macrozone, fourteen sites reported palaeotsunami deposits from a variety of different environments including coastal lakes, wetlands, and low terraces (Fig. 4) (e.

g. Atwater et al., 1992, 2013; Cisternas et al., 2005; Le Roux et al., 2008; Nelson et al., 2009; Morton et al., 2011; Garrett et al., 2015; Nentwig et al., 2015; Hong et al., 2016; Cisternas et al., 2017; Dura et al., 2017; Kempf et al., 2017; Nentwig et al., 2018; Brill and Cisternas, 2020; Kempf et al., 2020; Hocking et al., 2021). For example, sedimentary layers associated with tectonic subsidence and past-tsunami inundation were reported in the Maullín River (site #51) (Cisternas et al., 2005). Also, three studies (sites #55, 56 and 57) reconstructed 5500 and ~ 4300 years respectively, of tsunami records using long and continuous sediment cores and reflection-seismic profiles from two coastal lakes of Chiloe Island (e.g., Kempf et al., 2015, 2017, 2020). These sandy layers in the lacustrine record share sedimentological similarities with the 1960 tsunami deposits, thus supporting palaeotsunami interpretations. Another study, in Chucalén (site #52), recorded two extensive sandy layers in coastal marshes containing marine and brackish diatom assemblages indicating palaeotsunami inundations dated to 1270–1450 CE and 1070–1220 CE (Garrett et al., 2015). In addition, Nentwig et al. (2015) studied a sedimentary sequence in the Tirúa river marsh (site #42). Here, six tsunamigenic sand layers intercalated with fine-grained floodplain deposits were dated to 490 ± 110 CE, 530 ± 110 CE, 830–1250 CE, 1310 CE–1470 CE, 1730 ± 100 CE, and 1940 ± 10 CE (1960 Valdivia earthquake) by optically stimulated luminescence (OSL) on quartz. Other research used stratigraphic, lithologic, and diatom analyses to reconstruct land-level change records that showed variable coseismic slips coincident with three palaeotsunami inundations in 1470–1570 CE, 1425–1455 CE, and 270–410 CE in both Quidíco and Tirúa marshes (site #41) (Dura et al., 2017).

Similarly, Pliocene tsunami deposits have been inferred from sedimentary features in the southern macrozone. Le Roux et al. (2008) identified tsunami features such as sand dykes and sills injected into underlying cohesive muds, large blocks, rip-up intraclasts and structures resembling inverse gradation, planar laminae, as well as ripple and trough cross-lamination in the Huenteguapi sandstone (site #36, 37 and 38). The authors proposed that the backflow of a large Pliocene palaeotsunami (Goff et al., 2012a) eroded a coarse beach and coastal dunes, thus explaining the anomaly of coastal fauna within a continental shelf to slope environment.

Overall, palaeotsunami research within this macrozone has been shown to have significant potential, due to the presence of good tsunami indicators as well as suitable environments for identification like wetlands and marsh.

5.1.2.4. Deposits in the Austral macrozone. There are no palaeotsunami records reported from this zone within Chile. However, possible palaeotsunami evidence has been reported from the Atlantic coast of Argentina. At Ensenada de la Colonia (Fig. 1), erosional scarps and an overtopping fan architecture were detected by ground-penetrating radar. These facies changes were considered to represent at least three pulses of a unique tsunami episode that could be inferred, with the South Sandwich Islands subduction zone being a possible source (Bujalesky, 2012).

This zone is comprised largely of numerous small islands and the limited access to these areas restricts palaeotsunami research.

Table 4
Number of types of deposits in each category.

Category	Sites	Type of tsunami	Number of deposits
Four to five	#1–5, #7–8, #10, #12, #14–17, #20–34, #36, #39–48, #50–57	Modern	60
		Historic	22
		Palaeo	8
Two to three	#1–5, #7–10, #14, #18, #29, #35–42, #49–52, #54, #56–57	Historic	2
		Palaeo	62
One	#4–6, #10, #13, #29, #39, #49–51, #56–57	Paleo	23

5.2. The Chile tsunami deposit catalogue and qualitative assessment

The information from fifty-seven sites provides 178 deposits of modern, historic and palaeotsunami events (Table 3). After an analysis based on the criteria in Table 1, the results of the deposits were divided into three main groups. Table 4 summarises these findings.

The first group include ninety-one deposits that met four to five criteria. The results show that sixty describe modern tsunami deposits whose interpretations are well supported by instrumental measurements and eyewitnesses. In addition, twenty-two layers are linked to historic events. The physical features of these layers closely resemble their modern counterpart and numerical simulations reported in the area. The final eight layers only discuss palaeotsunami deposits. Their interpretation of palaeotsunami deposits is considered well-founded because of multiple interdisciplinary analyses to discard other potential high-energy wave sources. Also, the use of numerical models and correlation with other deposits permitted to associate them with a possible event that affected the area.

The second group include sixty-four deposits that met two to three criteria. Two of them are related to historic events interpreted by physical and cultural evidence, but there are no other deposits to correlate them. The rest are associated with palaeotsunami events, interpreted by multiproxy analyses that allow discriminating from other similar coastal floods as well as numerical simulations to estimate a possible source of the deposits. Also, a high portion is correlated with other deposits in other sites. In this category, some layers are validated by the original articles including the confidence levels of each of them.

Finally, twenty-three palaeotsunami deposits met one criterion due to controversy concerning the origins of the deposits. Also, there are a few correlations with other deposits, mainly assessed by geological analyses, and the original research assigned a low level of confidence to have been formed by a tsunami.

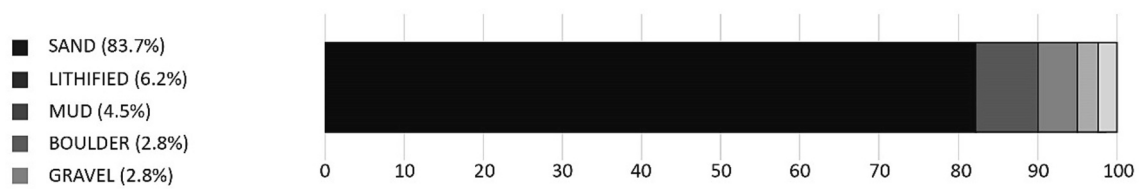
6. Present knowledge

6.1. Physical properties and emplacement mechanism for tsunami deposit

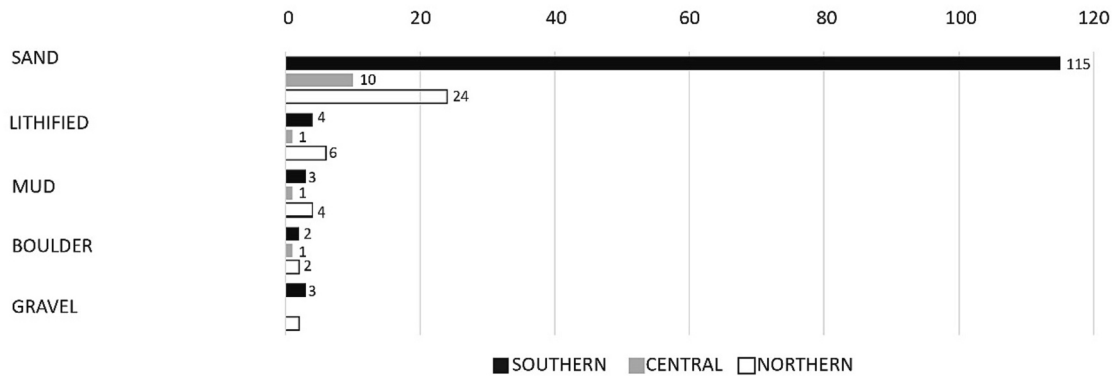
Tsunamis can cross entire ocean basins and transport a wide range of sediment sizes (e.g., Riou et al., 2020). A tsunami wave can therefore entrain sediments from any coastal environment and later deposit these as its energy wanes as it moves inland. Consequently, the grain size distribution of tsunami deposits very much depends on sediment source and availability (e.g., Fujiwara, 2008).

In Chile, tsunami deposits vary from layers of mud to boulders because of the wide diversity of coastal environments (rocky to soft-sediment coasts). Out of all the tsunami deposits studied in Chile, 84% are comprised of sandy layers (Fig. 5 a). The grain size distribution ranges from fine to coarse sand, although medium is the most common. These deposits have been recorded throughout Chile in onshore environments such as uplifted coastal plains, wetlands, lagoons, and estuaries (e.g., Cisternas et al., 2005; Dura et al., 2015; León et al., 2019; Kempf et al., 2020). One explanation for the predominance of sandy deposits is that most particles transported by tsunami waves are moved

a) Type of tsunami deposit in Chile



b) Types of deposits in each macrozone



c) Types of depositional environment in each macrozone

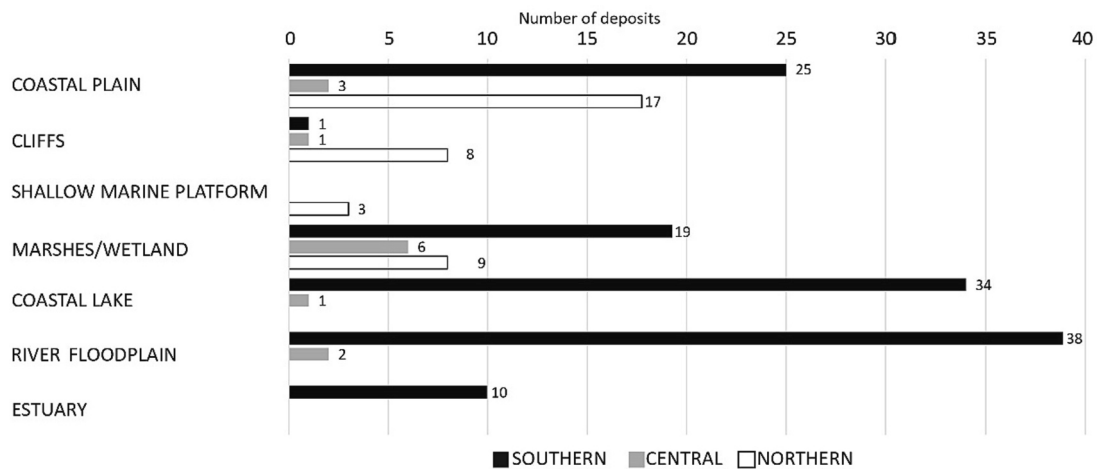


Fig. 5. Sedimentary characteristics and environment distribution of tsunami deposits in Chile. A) Overall percentages of grain-size distributions in tsunami evidence. B) The number of deposits of each grain size in every macrozone. C) The number of deposits in the most common environments where tsunami evidence can be recorded in each macrozone.

in the water column as suspension load and sand particles are small enough to be entrained in the water column and moved by convective and advective flows (Jaffe et al., 2007). Another possible explanation for this statistic is that most tsunami deposits that have been studied are concentrated in south-central Chile (38°S and 42°S), where exposed sandy beaches are the main source of sediments (Fig. 5 b) and in most cases, they are easily distinguishable from the rest of the stratigraphic profile (e.g., Cisternas et al., 2005; Dura et al., 2015). Sand deposits also contain more distinct sedimentary structures, which gives researchers information on the flow regime and direction that prevailed at the time of deposition in addition to insight into transport mode (Engel et al., 2020).

It is somewhat surprising that tsunamis recorded in lithified

sediments (sandstones and breccias) are the second most common type of deposit in Chile (6%). These deposits are the oldest records and suggest that large tsunamis affected extensive areas of the Chilean coast during the Plio-Pleistocene (e.g., Le Roux and Vargas, 2005; Le Roux et al., 2008) and Miocene (e.g., Cantalamessa and Di Celma, 2005; Le Roux, 2015). Importantly, tsunami deposits interpreted in lithified sediments can represent a major challenge to the determination of the generating process. Other high-energy phenomena such as mass flows and storms can leave similar sedimentary imprints, leading to considerable debate. For example, Cantalamessa and Di Celma (2005) reported on a tsunami deposit from the bay of Mejillones, but this interpretation was subsequently challenged by Bahlburg et al. (2010), who argued that the structural and sedimentological evidence would be better

interpreted as a debris flow associated with a small graben. Similarly, Spiske et al. (2014) challenged the interpretation of an apparent Pliocene tsunami backwash deposit at Hornitos in northern Chile (Hartley et al., 2001), arguing that it was a debris flow caused by an earthquake in the Andean subduction zone. In response to this reinterpretation, Le Roux (2015) suggested that a mass flow can also be caused by tsunami backwash events and would be difficult to distinguish from those caused by gravity alone, especially to the limited extent of the Hornitos outcrop.

Since lithified and unlithified deposits are not comparable and considering how distinct each modern marine tsunami deposit is (as observed from recent tsunami events such as the 2004 Indian Ocean Tsunami and the 2011 Japan tsunami), it is extremely difficult to establish a connection between these lithified deposits and tsunami behaviours. The sedimentary rocks identified as pre-Holocene tsunami deposits could also have been formed by mechanisms of other tsunamis, such as rock falls, landslides, and debris flows (Bahlburg et al., 2010). This exchange of arguments shows how sedimentary evidence on lithified rock may have different interpretations. Therefore, in these cases, it is crucial to carefully examine the sedimentary evidence that describes the physical properties of the phenomena and consider the secondary processes that may be involved with tsunamis. (Le Roux, 2015). Furthermore, to correlate the evidence with other sites and examine the number of different proxies that support the interpretation that for the case of lithified rock it could be limited by the stiffness of the rock.

Muddy tsunami deposits are less common in Chile, representing only 5% of those reported (Fig. 5 a). Only five studies have recorded this type of sediment, and these are attributed to both historical and palaeotsunamis in humid and calm environments (e.g., coastal lakes and estuarine) (e.g., Nelson et al., 2009; Kempf et al., 2020). A single muddy sediment record was identified from marine cores in the Mejillones' shallow marine basin (Vargas et al., 2005), where low energy conditions allowed for the identification of tsunami signals. The sediment characteristics included an angular unconformity, slumping and associated lenticular coarse-grained deposits generated because of local reworking of shallow water material. Mud caps are uncommon in the literature, but they should be present in suitable inland locations where the finest particles have been transported farther inland than their coarser counterparts (e.g., Goto et al., 2010). Furthermore, particle cohesion and resistance to post-deposition processes make them a reliable and resistant sedimentary feature (Spiske et al., 2013a). In summary, all the muddy tsunami deposits in Chile are found in low-energy and water-saturated environments, none have been reported in association with coarser-sized subaerial deposits.

Tsunami boulders represent around 3% of all tsunami evidence in Chile. Most of these records are associated with modern tsunamis in coastal plains or cliffs, such as those deposited by the 2010 and 2015 tsunamis. Only one record, in northern Chile, is associated with a palaeotsunami that probably occurred in the 15th century and is most likely linked with the "orphan event" of 1420 CE that affected Japan (Abad et al., 2020). Written records from Japan support the idea of a source located in northern Chile (Tsuji, 2013). In general, tsunami boulders are relatively uncommon in Chile, and have, not surprisingly, only been recorded in environments dominated by rocky coasts.

Finally, gravel deposits have only been described in four sites, around 3% of all layers. One of them was reported in Isla Mocha (38° S) following the 2010 tsunami. The gravels were mixed with sand and comprised less than 30% of the deposit (Bahlburg and Spiske, 2012). Some pebbles were imbricated toward the sea. These were concentrated around erosional gullies and were, therefore interpreted as backwash deposits. Also, in Los Hornos (site # 10) at the base of a palaeotsunami layer that was represented by a shear carpet in a channel with megaflutes (Le Roux and Vargas, 2005). Both structures indicate a turbulent flow followed by a dense, highly sheared fluid suggesting a tsunami source. Indeed, tsunami gravel deposits are not common and can sometimes be confused with river gravels. Therefore, it is crucial to match the deposits with other evidence such as fossil analyses to confirm

a marine source. On the other hand, if gravels are accompanied by other finer sediments, they can prove useful since they are often preserved in the sedimentary record far longer than sandy layers (Yamada et al., 2014). In addition, cobbles and gravel deposits can be imbricated, and thus reveal information on the direction of tsunami flow (e.g., Bahlburg and Spiske, 2012; León et al., 2019; Salazar et al., 2022).

6.2. Environmental condition and deposit preservations

This review has shown that most tsunami deposit records are concentrated in southern Chile. Indeed, 71% are in Southern Chile, 21% in the North, 8% in the Central area and none in Austral Chile (Fig. 5 a). It should be noted that the length of coastline for each macrozone varies considerably, with northern Chile covering almost 1700 km, Central 450 km, Southern 880 km, and Austral 2900 km.

Despite Austral Chile having the longest coastline, almost 50% of Chile's total coast length, no tsunami evidence has been reported. A possible explanation for this lack of record might be a change in the tectonic settings. Here the subducting plate changes to the Antarctic Plate and it moves under the South America Plate at a rate of only 18.5 mm per year, thereby tsunamigenic earthquakes are likely to be less frequent (Demets et al., 1994). In addition, the continent is fragmented into small islands and therefore, conducting tsunami research is limited by access. Because of the limited accommodation space, fjords in these regions do not develop large coastal plains where tsunami sediments could be deposited and trapped. It should be noted that high discharge from snowmelt and heavy precipitation due to surface runoff from rainwater floods also affect the potential for preservation (Bahlburg and Spiske, 2015). Despite this limitation, this area gathers the largest number of lagoons and lakes in the territory (Ministerio de Obras Públicas, 2015), which represent low-energy environments where tsunami deposits could preserve (e.g., Bondevik et al., 2005).

Almost three-quarters of tsunami deposits (71%) are in the southern Chile macrozone representing only 15% of Chile's coastline. The climate of southern Chile is a Warm-summer Mediterranean climate (Csb) and Oceanic climate (Cfb) (Fig. 2), both are characterized by high precipitations that allow the development of low-energy environments. The deposits recorded in this area were reported from coastal lakes, river mouths and marshes/wetlands (Fig. 5 c), where tsunami sediments are well preserved. In these environments, organic matter is abundant and within the stratigraphic sequence, tsunami deposits are characterized by light-coloured fine particles (mud to fine sand) mixed with dark-coloured organic matter. During tsunami inundation, the water and geomorphology of these environments function as barriers reducing the flow speed. Consequently, they create excellent conditions for deposition and "trapping" the sediments transported inland (Dawson et al., 2020). Following inundation, high sedimentation rates quickly bury tsunami layers, thus preserving and protecting them from post-depositional processes such as wind erosion and human disturbance (e.g., Kortekaas and Dawson, 2007; Ishimura and Miyauchi, 2015). Therefore, there is a distinct advantage in conducting tsunami surveys in these environments since the deposits can be clearly distinguished from the normal low-energy sediments (Spiske et al., 2013a). Nevertheless, it should be noted that subsequent soil development and vegetation growth on top of the tsunami deposits can alter the sediment structure and grain size within a few years (e.g., Bahlburg and Spiske, 2015; Spiske et al., 2020). Consequently, we emphasized that is important to consider post-depositional alterations to properly interpret the tsunami characteristics and thus avoid misleading interpretations.

An additional advantage is that it is relatively easy to collect samples for radiocarbon analyses from these sites because of the excellent preservation and abundance of organic matter. This helps to better constrain event ages and thus improve the reliability of the interpretations. In general, the level of confidence in tsunami deposits found in southern Chile is higher than elsewhere because: (1) of the possibility of performing multiple analyses that support a tsunami source, (2) of the high

quality of deposit preservation, and (3) they are easier to recognise in the stratigraphy.

Central Chile has a warm-summer Mediterranean climate (Csb), and this represents 7.5% of the country's coastline. This macrozone encompasses, 8% of all the tsunami records with most found in marshes/wetlands (Fig. 5c). However, there are also tsunami deposits found in low-lying coastal plains and river channels. Despite being wetlands, these environments are less protected and more susceptible to erosion than their southern counterparts, hence tsunami deposits are less well preserved. Only one site (#19) has evidence of palaeotsunami with the rest recording the 2010 tsunami. An explanation for these results is the lack of palaeotsunami research in the area in addition to high urbanization and anthropogenic alteration of some potential sites. It should be noted that in central Chile, most tsunami deposits are sandy layers interbedded with the local stratigraphy and there is only one that is muddy and another that is comprised of a boulder field. Again, the distribution of deposits in this macrozone is seemed to be controlled by the grain size of the source coupled with the effects of the local topography that allows the preservation of the deposits.

In contrast to these last macrozones, northern Chile presents by far the least favourable conditions to preserve recognisable tsunami deposits. The development of sediment traps is limited by prominent levels of aridity that promotes tsunami deposit erosion by winds and/or flash floods (Spiske et al., 2013a). However, 21% of the tsunami evidence has been reported in these conditions (Fig. 5 b). Most deposits reported along this coast are sandy layers because of the necessary concentration of studies along sandy beaches. Also, many of the onshore deposits documented in this area are from coastal plains or cliffs-tops (e.g., León et al., 2019; Abad et al., 2020) as opposed to coastal lakes and estuaries in the other zones (Fig. 5 c).

Furthermore, this macrozone tends to contain tsunami evidence comprised of boulders and lithified sediments (Fig. 5b). In general, these deposits can be preserved longer than the finer material in unconsolidated sediments (McAdoo et al., 2008). However, this was not the case on Isla Mocha where boulders disintegrated after they were transported onshore (Bahlburg and Spiske, 2015). In the same way, a disadvantage of these records is the difficulty to collect samples for multidisciplinary analyses (such as geochemistry and micro-fossil analyses). Another limitation is the complexity of obtaining adequate samples for dating, which makes it difficult to constrain the age of the events. Consequently, we have assigned lower validity values for tsunami records in boulders and sedimentary rocks than those in sandy sediments due to these limitations that can lead to cross-interpretation.

Importantly, the northern macrozone has significant sites where a palaeotsunami has been reported as a mud record in the Mejillones shallow basin. This evidence is important because it represents the only offshore evidence of tsunamis in Chile (Vargas et al., 2005), and opens an exciting avenue for future tsunami research.

Although gravel deposits are uncommon in Chile, Le Roux and Vargas (2005) interpreted a tsunami backwash by a layer of gravel at Los Hornos in the Atacama region (site #10 in Fig. 3). These sediments are part of a shear carpet structure at the base of a Plio-Pleistocene palaeotsunami, which suggests hyper-concentrated and highly sheared flows. As well as boulders, the advantage of tsunami gravel beds is their resistance to erosive processes, however, they may be confused with fluvial events (Yamada et al., 2014). To avoid confusion, it is necessary to identify other sedimentary structures indicative of tsunami flows, such as convex-up bivalves or megaflutes that allow the interpretation of hydrodynamics and flow direction. Despite these limitations, the gravel-rich coasts of northern Chile represent a significant unexplored area that has a high potential to record more tsunami deposits.

It should be noted that, in northern Chile, sandy tsunami layers are significantly fewer than in the southern macrozone (Fig. 5b). Although some sandy deposits were found (including some from the 2015 event), the aridity in this zone makes all sediment layers look remarkably similar (León et al., 2019), and as such tsunami deposits can be

overlooked. In these high arid conditions, both archaeological sites and small fluvial creeks can be remarkably good for preserving sandy palaeotsunami deposits (e.g., León Canales et al., 2019; Muñoz Cupitty, 2019; Salazar et al., 2022). Most of the archaeological sites along the coasts of northern Chile are located in areas protected from erosive effects such as waves and wind, allowing the preservation of tsunami deposits interbedded between well-preserved anthropogenic strata (Salazar et al., 2022). Also, on Chile's northern coast there are a small number of coastal wetlands and estuaries where tsunami evidence may be preserved (e.g., DePaolis et al., 2021; Easton et al., 2022), and should be explored further.

Tsunami studies have implemented methods following a multidisciplinary effort that supports the origin of a tsunami (e.g., Goff et al., 2012b) and geological approaches are the most used (Table 3). This trend can be explained in part by the fact that most of the tsunami deposits in Chile are unconsolidated sediments (layers of sand). In this context, grain size analyses are used to identify common characteristics of tsunamis, such as normal grading and the thinning of the layers inland (e.g., Cisternas et al., 2005; Dura et al., 2015; Bahlburg et al., 2018). However, geological data alone is insufficient to interpret tsunami deposits, so contextual information (historical data), identification of marine species and geochemical signatures have also been used. When used together these multiple lines of evidence reduce the chance of misinterpretation. Indeed, studies in Chile have shown that a multiproxy approach is essential to correctly interpret tsunami deposits.

In summary, most of the tsunami evidence in Chile is concentrated in the southern macrozone where low-energy environments (coastal lakes, river mouths and marshes/wetlands) are conducive to the deposition of sandy deposits. In the northern area, studies have identified tsunami evidence in coastal plains and cliffs where layers of sand and boulders were emplaced. Finally, the Central macrozone has the least number of deposits represented by a few sandy and muddy layers in marshes/wetlands.

6.3. Current record of major historical and prehistoric events

In general, historic tsunami deposits (Figs. 3 and 4) are remarkably scarce compared with the number of major tsunamigenic events that have occurred in Chile (Table 1). Only twelve out of thirty-one have been recorded by geological studies, with most of them found in Southern and Central Chile. An explanation for the low preservation of historic deposits records is the influence of early diagenetic processes (e.g., bioturbation and erosion) in the reduction of thickness and changes in the composition of these deposits, which in some cases can lead to a total disintegration (Spiske et al., 2013a).

The evidence in central and southern Chile is mostly associated with the 1960 and 2010 tsunamis, with some older tsunamis such as the one in 1575 CE. It should be noted that from almost all tsunamigenic earthquakes in southern Chile, tsunami deposits have been recorded in onshore environments, except for the 1570 CE event. An explanation for this might be the availability of historical records that validate a tsunami source. All these events were triggered by large earthquakes (>8.5 Mw) that caused significant impacts in populated areas, so there is a considerable amount of historical evidence describing inundations. This improves the level of confidence for these deposits, reflected in higher values. Another factor that affects the identification of historic tsunami records here is climatic conditions which allow better preservation of the deposits. Consequently, there are more sites where tsunami studies can be conducted and thus increasing the probability of finding deposits. Also, the largest earthquake in modern times occurred in southern Chile (Mw 9.5 in 1960) which has served to focus much of the research effort in this region as opposed to elsewhere in the country.

Conversely, in northern Chile, deposits from only five of the fourteen historic tsunamis have been recorded (Fig. 3). The deposits are all from the 2015 tsunami but are also layers likely associated with the 1604 CE, 1868 CE, 1877 CE and 1922 CE events. There is other evidence such as

shipwrecks in Arica and other tsunami deposits recorded in southern Peru (Spiske et al., 2013b), which can complement these records but in general, the number of records is scarce. Several reasons limit the correlation of deposits with tsunami events. First, the limited number of inhabited coastal areas in northern Chile directly affects the amount of historical evidence. Reports are only concentrated in a few of the main cities and many sites that could be affected by tsunamis have no written or eyewitness reports. Secondly, the high rate of aridity impedes the formation of sediment traps for tsunami inundation, consequently, this decreases the odds of finding deposits. Also, anthropogenic reworking may limit the preservation in the few sites where deposits have been identified (e.g., Bahlburg and Spiske, 2015). Despite this, our review has highlighted that there are a few low-energy environments in northern Chile that would benefit from further investigations (e.g., DePaolis et al., 2021; Easton et al., 2022), and it has also been demonstrated that archaeological sites also represent suitable locations for the preservation of tsunami deposits under arid conditions (e.g., León et al., 2019; Muñoz Cupitty, 2019). The high number of unrecorded events that have affected this zone makes it a particularly significant region for further research.

Palaeotsunami deposits are an important source of information that shows evidence of these events in the past and, based on the distribution of the deposits, major events can be identified, their frequency and tsunami gap could be estimated. In Chile, ninety-two palaeotsunami deposits have been identified, with events from the Miocene until Late Holocene.

Some of these events can be correlated according to their age and in northern Chile, two possible major events have been interpreted. By ~3800 years ago, geoarchaeological records showed a large tsunami that disrupted prehistoric societies, suggesting that the catastrophe was caused by a 1000 km long megathrust rupture (Salazar et al., 2022). Another event around 1420 CE has been identified in four sites from Mejillones until Pachingo spanning 800 km between the deposits (e.g., Vargas et al., 2005; Abad et al., 2020; DePaolis et al., 2021; Araya et al., 2022).

In Central and Southern Chile, multiple lines of evidence show a tsunami occurred around 1340 CE, based on correlation from sandy layer in wetland deposits in Tirúa and Maullín (e.g., Cisternas et al., 2005; Atwater et al., 2013; Garrett et al., 2015; Nentwig et al., 2015; Cisternas et al., 2017). Another event potentially occurred by 400 CE, correlated by at least three sites in Tirúa, Maullín, lake Cucao and Huelde (e.g., Nelson et al., 2009; Nentwig et al., 2015; Dura et al., 2017; Kempf et al., 2017, 2020).

It should be noted that tsunami deposits in sedimentary rock proposed a major event in the Miocene from deposits in northern Chile (e.g., Cantalamessa and Di Celma, 2005; Le Roux and Vargas, 2005), and another event has been reported from Antofagasta until Tirúa during Pliocene (e.g., Paskoff, 1991; Hartley et al., 2001; Le Roux et al., 2008; Le Roux, 2015). Some authors indicate that these deposits are likely related to the Eltanin impact (Goff et al., 2020), while others argue that the observed grain sizes of these deposits are much too large to have been transported by the Eltanin tsunami (Weiss et al., 2015).

7. Potential ways forward

7.1. The likelihood of finding the parents of orphan tsunamis along Chile's coast

The study of tsunami deposits allows researchers to identify events that have happened in the past. Among them are, those historical tsunamis reported with no "parental" earthquake or other tsunami-generating sources identified and these are known as "Orphan tsunamis." The 1700 CE Cascadia event is a famous example, where unusual waves inundated the shores of Japan, but the parental earthquake was only identified in the 1980s by correlating tsunami deposits in Japan with evidence of a large earthquake in North America's Cascadia

region (Atwater et al., 2005). This conclusion is partly built on the identification of far-travelled waves of historical tsunamis that inundated the coast of Japan.

Numerous tsunamis generated by historical earthquakes in Chile have also been observed in Japan (e.g., Valparaíso 1730 CE, Concepción 1751 CE, Iquique 1877 CE, Valdivia 1960 CE, etc.) (e.g., Goff et al., 2022). Water levels at the shore or on land were mentioned in historical texts or measured from physical tsunami damage. It should be noted that the tide level at the time of the tsunami's arrival at the coast must be considered in order to determine the precise tsunami heights. If the date and time are known, the tide level may be calculated using the current tide harmonics. Therefore, far-field records are an important piece of evidence to resemble the origin of orphan tsunamis (Satake et al., 2020). The same approach could be used to find the parents of other orphan tsunamis on the coast of Chile. For instance, a historical report from Japan described a tsunami in 1420 CE at the coast of Kawagoro Aise (Aise fishery port, Hitachi City, Ibaraki Prefecture) with waves up to two metres high (Iida et al., 1967). No earthquake was felt locally, so it is considered that it may relate to a distant tsunami that could have come from Chile (Tsuji, 2013). In Chile, the chronicles related to tsunamis date only started in the 16th Century (Lomnitz, 1970), therefore this event is beyond historical records. Therefore, the identification of palaeotsunami deposits in northern Chile represents remarkable evidence in helping to understand the 1420 CE event. On the coast of the Atacama Region, large boulders were deposited on an 18.5 m-high cliff and radiocarbon dates suggest a correlation with the 1420 CE tsunami (Abad et al., 2020). Further north in Mejillones Bay, an angular unconformity and lenticular coarse grain layer from short shallow marine sediment cores were interpreted as the result of an earthquake that occurred between 1408 and 1449 CE (Vargas et al., 2011). In Arica and Tongoy, layers of medium to coarse sand with sharp basal contact, erosive channels, cross and slip bedding, and rip-up clasts were identified in archaeological sites and wetlands, likely related to the same event (Easton et al., 2022; Muñoz Cupitty, 2019; unpublished results).

In addition, palaeotsunami layers dated within the age range of this event have been recorded across the Pacific Ocean, with a suggested earthquake origin associated with the Tonga trench (Goff et al., 2022). According to the tsunami magnitude formula (Carvajal et al., 2017b), an earthquake's $M_w > 9$ is required for a tsunami to travel across the Pacific Ocean with an amplitude of more than 1 m. Tsunami waves smaller than this are within the range of ocean tide and therefore unlikely to be recorded in pre-instrumental historical records or geological strata (Satake et al., 2020). While alternative tsunamigenic sources have been proposed (e.g., Goff et al., 2012b; Butler et al., 2017a, 2017b; Goff et al., 2020), these do not exclude the possibility that they could relate to an orphan tsunami around 1420 CE, and the source could be from northern Chile.

Given the number of proposed tsunamigenic sources, additional studies are needed along the coast of northern Chile that consider the difference between near and far-field tsunamis, as well as numerical simulation of tsunamis to test the different scenarios in concordance with inverse simulations based on the deposits (e.g., Sugawara et al., 2019; Bosnic et al., 2021; Nakanishi and Ashi, 2022), and thus identify the possible sources of orphan tsunamis.

7.2. Landslides as a source of tsunamis deposits in Chile

This review has shown that the main source of tsunami deposits in Chile are megathrust earthquakes in the subduction zone along the Peru-Chile Trench. Besides, according to National Oceanic and Atmospheric Administration (2022) landslides are the second most common cause. In Chile, few studies report tsunamis triggered by landslides and most of them are associated with historical events. For example, in 1965, a debris flow caused by the collapse of the Yate volcano in southern Chile flowed 7500 m along the shores of Lake Cabrera, causing a tsunami that killed twenty-seven people. Field data estimated wave heights of 25 m

and up to 50 m southwest of the shore (Watt et al., 2009). Also, on 21 April 2007, an Mw 6.2 earthquake caused hundreds of landslides along the sides of the Aysén fjord. Some landslides moved material underwater, producing a series of tsunamis within the fjord (e.g., Sepúlveda et al., 2010; Lastras et al., 2013). Importantly, Mather et al. (2014) reported more than sixty late Neogene coastal landslides across the hyper-arid Coastal Cordillera of the Atacama Desert of northern Chile. Most of them reached the Pacific Ocean coast, representing a potential source of tsunamis within one of the most important seismic gaps of South America.

In conclusion, these examples show that landslides are an important tsunamigenic source in Chile. These can occur in both coastal environments and lakes. This is an unexplored area of research that could contribute to expanding the records of tsunamis in Chile, especially in the Austral zone where the influence of the Liquiñe-Ofqui Fault Zone (Fig. 4) is considered a source of earthquakes that can trigger landslides (Russo et al., 2011).

7.3. Palaeotsunami research for tsunami hazard assessment in Chile

The hazard of tsunamis on the Chilean coast is significant given the high frequency of these events during modern, historical, and prehistoric times. For example, tsunami evidence in archaeological sites of Taltal has revealed that the impacts of Holocene palaeotsunamis were greater than any known historical event, presenting a picture of major tsunami inundation in northern Chile (León et al., 2019). Likewise, the study of boulder deposits on an 18 m high cliff on the coast of the Atacama Desert has been identified as possible evidence for the 1420 CE orphan tsunami recorded in Japan (Abad et al., 2020), strengthening the hypothesis that its source could be located off the coast of northern Chile. In addition, plenty of palaeotsunami deposits in different environments (coastal lakes, wetlands and coastal plain) along southern Chile has allowed us to extend the tsunami history of areas affected by the 1960 CE great earthquake. This information is crucial in helping to estimate the recurrence intervals of large tsunamis based on historical and geological evidence, and thus allows us to be better prepared for future events. If proof is needed of this, then the geological studies conducted in Japan before the 2011 Tōhoku-Oki tsunami, found deposits of the precursor 869 CE Jōgan tsunami which indicated a far worst scenario for the region. As mentioned by Sawai et al. (2012), this geological research could have been and should be used to improve tsunami hazard assessment including evacuation maps and awareness public information.

In Chile, tsunami flood charts (CITSU in Spanish) have been developed by SHOA since 1997 and define the maximum flood levels expected for the main urban and port areas. These maps use the “COMCOT” numerical model which in most cases considers parameters based on the worst historical tsunami that has affected each zone. This information is used in urban planning and preparation for civil evacuation. Nevertheless, palaeotsunami records are not considered for these maps. If used then they could lead to better prevention, especially in some areas where studies have demonstrated that prehistoric tsunamis were larger than those in historic times (e.g. León et al., 2019; Salazar et al., 2022). Undoubtedly, the recognition of tsunami deposits represents an important piece of information that can be used to improve tsunami hazard assessment for Chile.

8. Final remarks

This review paper has presented a broad chronological and geographical overview of tsunami imprints in the coastal environments of Chile. Due to the high frequency of tsunamis, many types of deposits have been found to reveal crucial information to help better understand tsunami behaviour. Tsunami deposits in Chile range from modern to historical and palaeoevents. Most tsunami deposits that have been found are concentrated in southern Chile largely because of favourable

climatic conditions that aid in the development of low-energy environments which help preserve the depositional evidence. The deposits are mainly associated with layers of sand that contrast well with the rest of the stratigraphic sequence. In northern Chile, an arid climatic condition prevents the development of geomorphological traps in conjunction with geomorphology that is dominated by rocky coasts. However, studies have been able to identify tsunami deposits associated with archaeological sites and as cliff-top boulders. This review has highlighted the importance of emerging areas in tsunami research and summarised the major findings to date, providing a detailed spatial distribution and explaining the evidence used to support a tsunami origin.

Chile represents a suitable place to conduct tsunami research and this review has summarised the available data. The data can be used as a guide not only to identify unexplored areas but also to help understand the type of deposits that may be found in climatic macrozones along the coast of Chile.

Finally, we have pointed out that tsunami hazard assessment in Chile relies on models that use only historical data. The further development of tsunami sediment transport models based on sedimentary and associated information from palaeotsunami deposits will allow far more realistic assessments of the tsunami hazard for the coast of Chile. Therefore, we recommend that palaeotsunami data along with inverse numerical models be included in the tsunami hazard assessment to improve preventive measures against future events on the Chilean coast. We also recommend the use of numerical models to help identify coastal sites where tsunamis may cause significant inundation so that detailed geological studies can be conducted.

Declaration of Competing Interest

The authors acknowledge that there are no conflicts of interest recorded.

Data availability

All data are available in the main text and supplementary materials.

Acknowledgements

This research was supported in part by the project Fondecyt # 1201387. The first author is benefited from ANID (Conicyt) through Doctoral Grants. This work is a contribution to IGCP Project 725 ‘Forecasting Coastal Change’.

Appendix A. Supplementary data

Supplementary data to this article can be found online at <https://doi.org/10.1016/j.earscirev.2022.104273>.

References

- Abad, M., Izquierdo, T., Cáceres, M., Bernárdez, E., Rodríguez-Vidal, J., 2020. Coastal boulder deposit as evidence of an ocean-wide prehistoric tsunami originated on the Atacama Desert coast (northern Chile). *Sedimentology* 67 (3), 1505–1528. <https://doi.org/10.1111/sed.12570>.
- Abe, K., 1979. Size of great earthquakes of 1837–1974 inferred from tsunami data. *J. Geophys. Res. Solid Earth* 84 (B4), 1561–1568. <https://doi.org/10.1029/JB084iB04p01561>.
- Aránguiz, R., Shibayama, T., Yamazaki, Y., 2014. Tsunamis from the Arica-Tocopilla source region and their effects on ports of Central Chile. *Nat. Hazards* 71 (1), 175–202. <https://doi.org/10.1007/s11069-013-0906-5>.
- Aránguiz, R., González, G., González, J., Catalán, P.A., Cienfuegos, R., Yagi, Y., Okuwaki, R., Urrea, L., Contreras, K., Del Río, I., Rojas, C., 2015. The 16 September 2015 Chile tsunami from the post-tsunami survey and numerical modeling perspectives. *Pure Appl. Geophys.* 173 (2), 333–348. <https://doi.org/10.1007/s00024-015-1225-4>.
- Araya, K., Muñoz, P., Dezileau, L., Maldonado, A., Campos-Caba, R., Rebolledo, L., Cardenas, P., Salamanca, M., 2022. Extreme sea surges, Tsunamis and pluvial flooding events during the last~ 1000 years in the semi-arid Wetland, Coquimbo Chile. *Geosciences* 12 (3), 135.

- Atwater, B.F., Nunez, H.J., Vita-Finzi, C., 1992. Net Holocene emergence despite earthquake-induced submergence, south-central Chile. *Quat. Int.* 15 (16), 9.
- Atwater, B.F., Musumi-Rokkaku, S., Satake, K., Tsuji, Y., Ueda, K., Yamaguchi, D.K., 2005. The orphan tsunami of 1700—Japanese clues to a parent earthquake in North America (1707). Retrieved from <http://pubs.er.usgs.gov/publication/pp1707>.
- Atwater, B.F., Cisternas, M., Yulianto, E., Prendergast, A.L., Jankaew, K., Eipert, A.A., Fernando, W.L.S., Tejakusuma, I., Schiappacasse, I., Sawai, Y., 2013. The 1960 tsunami on beach-ridge plains near Maullín, Chile: Landward descent, renewed breaches, aggraded fans, multiple predecessors. *Andean Geol.* 40 (3) <https://doi.org/10.5027/andgeoV40n3-a01>.
- Bahlburg, H., Spiske, M., 2012. Sedimentology of tsunami inflow and backflow deposits: key differences revealed in a modern example. *Sedimentology* 59 (3), 1063–1086. <https://doi.org/10.1111/j.1365-3091.2011.01295.x>.
- Bahlburg, H., Spiske, M., 2015. Styles of early diagenesis and the preservation potential of onshore tsunami deposits—Are-survey of Isla Mocha, Central Chile, 2 years after the February 27, 2010, Maule tsunami. *Sediment. Geol.* 326, 33–44. <https://doi.org/10.1016/j.sedgeo.2015.06.009>.
- Bahlburg, H., Spiske, M., Weiss, R., 2010. Comment on “Sedimentary features of tsunami backwash deposits in a shallow marine Miocene setting, Mejillones Peninsula, northern Chile” by G. Cantalamessa and C. Di Celma [Sedimentary Geology 178 (2005) 259–273]. *Sediment. Geol.* 228 (1), 77–80. <https://doi.org/10.1016/j.sedgeo.2010.03.006>.
- Bahlburg, H., Nentwig, V., Kreutzer, M., 2018. The September 16, 2015 Illapel tsunami, Chile – Sedimentology of tsunami deposits at the beaches of La Serena and Coquimbo. *Mar. Geol.* 396, 43–53. <https://doi.org/10.1016/j.margeo.2016.12.011>.
- Barrientos, S., 1980. Regionalización sísmica de Chile. Memoria para optar al grado de Magister en Ciencias con Mención en Geofísica. Universidad de Chile, Santiago, Chile.
- Barra, R., Cisternas, M., Suarez, C., Araneda, A., Pinones, O., Popp, P., 2004. PCBs and HCHs in a salt-marsh sediment record from South-Central Chile: use of tsunami signatures and ¹³⁷Cs fallout as temporal markers. *Chemosphere* 55 (7), 965–972. <https://doi.org/10.1016/j.chemosphere.2003.12.006>.
- Bellanova, P., Bahlburg, H., Nentwig, V., Spiske, M., 2016. Microtextural analysis of quartz grains of tsunami and non-tsunami deposits – a case study from Tirúa (Chile). *Sediment. Geol.* 343, 72–84. <https://doi.org/10.1016/j.sedgeo.2016.08.001>.
- Bondevik, S., Løvholt, F., Harbitz, C., Mangerud, J., Dawson, A., Svendsen, J.I., 2005. The Storegga Slide tsunami—Comparing field observations with numerical simulations. In: Ormen lange—an integrated study for safe field development in the storegga submarine area. Elsevier, pp. 195–208.
- Borrero, J.C., Goring, D.G., 2015. South American Tsunamis in Lyttelton Harbor, New Zealand. *Pure Appl. Geophys.* 172 (3), 757–772. <https://doi.org/10.1007/s00024-014-1026-1>.
- Bosnic, I., Costa, P.J.M., Dourado, F., La Selle, S., Gelfenbaum, G., 2021. Onshore flow characteristics of the 1755 CE Lisbon tsunami: linking forward and inverse numerical modeling. *Mar. Geol.* 434, 106432 <https://doi.org/10.1016/j.margeo.2021.106432>.
- Brill, D., Cisternas, M., 2020. Testing quartz and feldspar luminescence dating to determine earthquake and tsunami recurrence in the area of the giant 1960 Chile earthquake. *Quat. Geochronol.* 58, 101080 <https://doi.org/10.1016/j.quageo.2020.101080>.
- Bujalesky, G.G., 2012. Tsunami Overtopping Fan and erosive scarps at Atlantic Coast of Tierra Del Fuego. *J. Coast. Res.* 28 (2) <https://doi.org/10.2112/JCOASTRES-D-11-00037.1>, 442–456, 415. Retrieved from.
- Butler, R., Burney, D.A., Rubin, K.H., Walsh, D., 2017a. The orphan Sanriku tsunami of 1586: new evidence from coral dating on Kaua ‘i. *Nat. Hazards* 88 (2), 797–819.
- Butler, R., Walsh, D., Richards, K., 2017b. Extreme tsunami inundation in Hawai ‘i from Aleutian-Alaska subduction zone earthquakes. *Nat. Hazards* 85 (3), 1591–1619.
- Campos-Caba, R., Beya, J., 2015. Cuantificación de los daños históricos a infraestructura costera por marejadas en las costas de Chile.
- Cantalamessa, G., Di Celma, C., 2005. Sedimentary features of tsunami backwash deposits in a shallow marine Miocene setting, Mejillones Peninsula, northern Chile. *Sediment. Geol.* 178 (3–4), 259–273. <https://doi.org/10.1016/j.sedgeo.2005.05.007>.
- Carvajal, M., Cisternas, M., Catalán, P.A., 2017a. Source of the 1730 Chilean earthquake from historical records: Implications for the future tsunami hazard on the coast of Metropolitan Chile. *J. Geophys. Res. Solid Earth* 122 (5), 3648–3660. <https://doi.org/10.1002/2017jb014063>.
- Carvajal, M., Cisternas, M., Gubler, A., Catalán, P.A., Winckler, P., Wesson, R.L., 2017b. Reexamination of the magnitudes for the 1906 and 1922 Chilean earthquakes using Japanese tsunami amplitudes: Implications for source depth constraints. *J. Geophys. Res.* 122, 4–17. <https://doi.org/10.1002/2016JB013269>.
- CERESIS, 1985a. Catálogo de terremotos para América del Sur, Chile, datos de hipocentros e intensidades.
- CERESIS, 1985b. Terremotos destructivos en América del Sur 1530-1894.
- Chagué-Goff, C., Goff, J., Wong, H., Cisternas, M., 2015. Insights from geochemistry and diatoms to characterise a tsunami’s deposit and maximum inundation limit. *Mar. Geol.* 359 <https://doi.org/10.1016/j.margeo.2014.11.009>.
- Chagué, C., Sugawara, D., Goto, K., Goff, J., Dudley, W., Gadd, P., 2018. Geological evidence and sediment transport modelling for the 1946 and 1960 tsunamis in Shinmachi, Hilo, Hawaii. *Sediment. Geol.* 364, 319–333. <https://doi.org/10.1016/j.sedgeo.2017.09.010>.
- Cisternas, M., Contreras, I., Araneda, A., 2000. Reconocimiento y caracterización de las facies sedimentarias depositadas por el tsunami de 1960 en el estuario Maullín, Chile.
- Cisternas, M., Atwater, B.F., Torrejon, F., Sawai, Y., Machuca, G., Lagos, M., Eipert, A., Youtlon, C., Salgado, I., Kamataki, T., Shishikura, M., Rajendran, C.P., Malik, J.K., Rizal, Y., Husni, M., 2005. Predecessors of the giant 1960 Chile earthquake. *Nature* 437 (7057), 404–407. <https://doi.org/10.1038/nature03943>.
- Cisternas, M., Torrejón, F., Gorigoitia, N., 2012. Amending and complicating Chile’s seismic catalog with the Santiago earthquake of 7 August 1580. *J. S. Am. Earth Sci.* 33 (1), 102–109. <https://doi.org/10.1016/j.jsames.2011.09.002>.
- Cisternas, M., Garrett, E., Wesson, R., Dura, T., Ely, L.L., 2017. Unusual geologic evidence of coeval seismic shaking and tsunamis shows variability in earthquake size and recurrence in the area of the giant 1960 Chile earthquake. *Mar. Geol.* 385, 101–113. <https://doi.org/10.1016/j.margeo.2016.12.007>.
- Comte, D., Pardo, M., 1991. Reappraisal of great historical earthquakes in the northern Chile and southern Peru seismic gaps. *Nat. Hazards* 4 (1), 23–44. <https://doi.org/10.1007/BF00126557>.
- Contreras, M., Winckler, P., Sepulveda, I., Andaur-Álvarez, A., Cortes, F., Guerrero, C., Mizobe, C., Iguait, F., Breuer, W., Beya, J., Vergara, H., Sterquel, R., 2016. Field survey of the 2015 Chile Tsunami with emphasis on coastal wetland and conservation areas. *Pure Appl. Geophys.* 173 <https://doi.org/10.1007/s00024-015-1235-2>.
- Costa, P., Silva, D., Figueirinhas, L., Lario, J., 2019. The importance of coastal geomorphological setting as a controlling factor on microtextural signatures of the 2010 Maule (Chile) tsunami deposit, Vol. 17.4.
- Costa, P.J.M., Andrade, C., Pufahl, P., 2020. Tsunami deposits: present knowledge and future challenges. *Sedimentology* 67 (3), 1189–1206. <https://doi.org/10.1111/sed.12724>.
- Dawson, S., Costa, P.J., Dawson, A., Engel, M., 2020. Onshore archives of tsunami deposits. In: Geological Records of Tsunamis and Other Extreme Waves. Elsevier, pp. 95–111.
- de Ballore, F. d. M., 1913. Historia sísmica de los andes meridionales al sur del paralelo XVI. Paper presented at the Anales de la Universidad de Chile.
- Demets, C., Gordon, R., Argus, D., Stein, S., 1994. Effect of recent revisions to the geomagnetic reversal time-scale on estimates of current plate motions. *Geophys. Res. Lett.* 21 <https://doi.org/10.1029/94GL02118>.
- DePaolis, J.M., Dura, T., MacInnes, B., Ely, L.L., Cisternas, M., Carvajal, M., Tang, H., Fritz, H.M., Mizobe, C., Wesson, R.L., Figueroa, G., Brennan, N., Horton, B.P., Pilarczyk, J.E., Corbett, D.R., Gill, B.C., Weiss, R., 2021. Stratigraphic evidence of two historical tsunamis on the semi-arid coast of north-central Chile. *Quat. Sci. Rev.* 266, 107052 <https://doi.org/10.1016/j.quascirev.2021.107052>.
- Deschamps, A., 1980. Mise au point sur les méthodes de calcul de sismogrammes synthétiques de longue période.
- Donnelly, J., Goff, J., Chagué-Goff, C., 2017. A record of local storms and trans-Pacific tsunamis, eastern Banks Peninsula, New Zealand. *The Holocene* 27 (4), 496–508.
- Dorbath, L., Cisternas, A., Dorbath, C., 1990. Quantitative assessment of great earthquakes in Peru. *Bull. Seismol. Soc. Am.* 80, 551–576.
- Dura, T., Cisternas, M., Horton, B.P., Ely, L.L., Nelson, A.R., Wesson, R.L., Pilarczyk, J.E., 2015. Coastal evidence for Holocene subduction-zone earthquakes and tsunamis in central Chile. *Quat. Sci. Rev.* 113, 93–111. <https://doi.org/10.1016/j.quascirev.2014.10.015>.
- Dura, T., Horton, B.P., Cisternas, M., Ely, L.L., Hong, I., Nelson, A.R., Wesson, R.L., Pilarczyk, J.E., Parnell, A.C., Nikitina, D., 2017. Subduction zone slip variability during the last millennium, south-central Chile. *Quat. Sci. Rev.* 175, 112–137. <https://doi.org/10.1016/j.quascirev.2017.08.023>.
- Easton, G., González-Alfaro, J., Villalobos, A., Álvarez, G., Melgar, D., Ruiz, S., Sepúlveda, B., Escobar, M., León, T., Carlos Báez, J., Izquierdo, T., Forch, M., Abad, M., 2022. Complex rupture of the 2015 Mw 8.3 Illapel earthquake and prehistoric events in the Central Chile Tsunami Gap. *Seismol. Res. Lett.* <https://doi.org/10.1785/0220210283>.
- Ely, L.L., Cisternas, M., Wesson, R.L., Dura, T., 2014. Five centuries of tsunamis and land-level changes in the overlapping rupture area of the 1960 and 2010 Chilean earthquakes. *Geology* 42 (11), 995–998. <https://doi.org/10.1130/g35830.1>.
- Engel, M., Pilarczyk, J., May, S.M., Brill, D., Garrett, E., 2020. Geological Records of Tsunamis and Other Extreme Waves. Elsevier, Amsterdam, Netherlands, Cambridge, MA.
- Fernandez, M.A., 2007. Arica 1868: un tsunami y un terremoto.
- Fritz, H.M., Petroff, C.M., Catalán, P.A., Cienfuegos, R., Winckler, P., Kalligeris, N., Weiss, R., Barrientos, S.E., Meneses, G., Valderas-Bermejo, C., Ebeling, C., Papadopoulos, A., Contreras, M., Almar, R., Dominguez, J.C., Synolakis, C.E., 2011. Field survey of the 27 February 2010 Chile Tsunami. *Pure Appl. Geophys.* 168 (11), 1989–2010. <https://doi.org/10.1007/s00024-011-0283-5>.
- Fujiwara, O., 2008. Chapter 4 - Bedforms and sedimentary structures characterizing tsunami deposits. In: Shiki, T., Tsuji, Y., Yamazaki, T., Nanayama, F. (Eds.), *Tsunamiites*, Second edition. Elsevier, pp. 53–64.
- Garrett, E., Shennan, I., Hocking, E., Woodroffe, S., 2013. Reconstructing paleoseismic deformation, 1: modern analogues from the 1960 and 2010 Chilean great earthquakes. *Quat. Sci. Rev.* 75, 11–21. <https://doi.org/10.1016/j.quascirev.2013.04.007>.
- Garrett, E., Shennan, I., Woodroffe, S.A., Cisternas, M., Hocking, E.P., Gulliver, P., 2015. Reconstructing paleoseismic deformation, 2: 1000 years of great earthquakes at Chucalen, south central Chile. *Quat. Sci. Rev.* 113, 112–122. <https://doi.org/10.1016/j.quascirev.2014.10.010>.
- Goff, J., Chagué-Goff, C., Archer, M., Dominey-Howes, D., Turney, C., 2012a. The Eltanin asteroid impact: possible South Pacific palaeomegatsunami footprint and potential implications for the Pliocene–Pleistocene transition. *J. Quat. Sci.* 27 (7), 660–670.
- Goff, J., Chagué, C., Nichol, S., Jaffe, B., Dominey-Howes, D., 2012b. Progress in palaeotsunami research. *Sediment. Geol.* s 243–244, 70–88. <https://doi.org/10.1016/j.sedgeo.2011.11.002>.
- Goff, J., Witter, R., Terry, J., Spiske, M., 2020. Palaeotsunamis in the Sino-Pacific region. *Earth Sci. Rev.* 210, 103352 <https://doi.org/10.1016/j.earscirev.2020.103352>.

- Goff, J., Borrero, J., Easton, G., 2022. In search of Holocene trans-Pacific palaeotsunamis. *Earth Sci. Rev.* 233, 104194 <https://doi.org/10.1016/j.earscirev.2022.104194>.
- Goto, K., Miyagi, K., Kawamata, H., Imamura, F., 2010. Discrimination of boulders deposited by tsunamis and storm waves at Ishigaki Island, Japan. *Mar. Geol.* 269 (1), 34–45. <https://doi.org/10.1016/j.margeo.2009.12.004>.
- Hartley, A., Howell, J., Mather, A.E., Chong, G., 2001. A possible Plio-Pleistocene tsunami deposit, Hornitos, northern Chile. *Rev. Geol. Chile* 28 (1), 117–125. <https://doi.org/10.4067/S0716-02082001000100007>.
- Horton, B.P., Sawai, Y., Hawkes, A.D., Witter, R.C., 2011. Sedimentology and paleontology of a tsunami deposit accompanying the great Chilean earthquake of February 2010. *Mar. Micropaleontol.* 79 (3–4), 132–138. <https://doi.org/10.1016/j.marmicro.2011.02.001>.
- Hocking, E.P., Garrett, E., Aedo, D., Carvajal, M., Melnick, D., 2021. Geological evidence of an unreported historical Chilean tsunami reveals more frequent inundation. *Commun. Earth Environ.* 2 (1), 245. <https://doi.org/10.1038/s43247-021-00319-z>.
- Hong, I., Dura, T., Ely, L.L., Horton, B.P., Nelson, A.R., Cisternas, M., Nikitina, D., Wesson, R.L., 2016. A 600-year-long stratigraphic record of tsunamis in south-central Chile. *The Holocene* 27 (1), 39–51. <https://doi.org/10.1177/0959683616646191>.
- Iida, K., Cox, D.C., Pararas-Carayannis, G., 1967. Preliminary Catalog of Tsunamis Occurring in the Pacific Ocean. Hawaii Institute of Geophysics, University of Hawaii, Honolulu.
- Ishimura, D., Miyauchi, T., 2015. Historical and paleo-tsunami deposits during the last 4000 years and their correlations with historical tsunami events in Koyadori on the Sanriku Coast, northeastern Japan. *Progr. Earth Planet. Sci.* 2 (1) <https://doi.org/10.1186/s40645-015-0047-4>.
- Jaffe, B., Dekker, F., Gelfenbaum, G., Vatvani, D., 2007. Coastal Sediments '07, pp. 1117–1128.
- Kausel, E., 1986. Los terremotos de agosto de 1868 y mayo de 1877 que afectaron el sur del Perú y norte de Chile. *Boletín de la Academia Chilena de Ciencias* 3 (1), 8–13.
- Kausel, E., Ramirez, D., 1992. Relaciones entre parámetros focales y macrosísmicos de grandes terremotos chilenos. *Revista Geofísica* 37, 36–194.
- Kempf, P., Moernaut, J., Van Daele, M., Vermassen, F., Vandoorne, W., Pino, M., Urrutia, R., Schmidt, S., Garrett, E., De Batist, M., 2015. The sedimentary record of the 1960 tsunami in two coastal lakes on Isla de Chiloé, south Central Chile. *Sediment. Geol.* 328, 73–86. <https://doi.org/10.1016/j.sedgeo.2015.08.004>.
- Kempf, P., Moernaut, J., Van Daele, M., Vandoorne, W., Pino, M., Urrutia, R., De Batist, M., 2017. Coastal lake sediments reveal 5500 years of tsunami history in south central Chile. *Quat. Sci. Rev.* 161, 99–116. <https://doi.org/10.1016/j.quascirev.2017.02.018>.
- Kempf, P., Moernaut, J., Van Daele, M., Pino, M., Urrutia, R., De Batist, M., 2020. Paleotsunami record of the past 4300 years in the complex coastal Lake system of Lake Cucao, Chiloé Island, south central Chile. *Sediment. Geol.* 401 <https://doi.org/10.1016/j.sedgeo.2020.105644>.
- Kortekaas, S., Dawson, A.G., 2007. Distinguishing tsunami and storm deposits: an example from Martinhal, SW Portugal. *Sediment. Geol.* 200 (3–4), 208–221.
- Lario, J., Zazo, C., Goy, J.L., 2016. Tectonic and morphosedimentary features of the 2010 Chile earthquake and tsunami in the Arauco Gulf and Mataquito River (Central Chile). *Geomorphology* 267, 16–24. <https://doi.org/10.1016/j.geomorph.2016.05.019>.
- Lastras, G., Amblas, D., Calafat, A.M., Canals, M., Frigola, J., Hermanns, R.L., Lafuerza, S., Longva, O., Micallef, A., Sepúlveda, S.A., 2013. Landslides cause tsunami waves: insights from Aysén fjord, Chile. *EOS Trans. Am. Geophys. Union* 94 (34), 297–298.
- Lau, A.Y.A., Switzer, A.D., Dominey-Howes, D., Aitchison, J.C., Zong, Y., 2010. Written records of historical tsunamis in the northeastern South China Sea – challenges associated with developing a new integrated database. *Nat. Hazards Earth Syst. Sci.* 10 (9), 1793–1806. <https://doi.org/10.5194/nhess-10-1793-2010>.
- Le Roux, J.P., 2015. A critical examination of evidence used to re-interpret the Hornitos mega-breccia as a mass flow deposit caused by cliff failure. *Andean Geol.* 42 (1) <https://doi.org/10.5027/andgeoV42n1-a08>.
- Le Roux, J.P., Vargas, G., 2005. Hydraulic behavior of tsunami backflows: insights from their modern and ancient deposits. *Environ. Geol.* 49 (1), 65–75. <https://doi.org/10.1007/s00254-005-0059-2>.
- Le Roux, J.P., Nielsen, S.N., Kemnitz, H., Henriquez, Á., 2008. A Pliocene mega-tsunami deposit and associated features in the Ranquil Formation, southern Chile. *Sediment. Geol.* 203 (1–2), 164–180. <https://doi.org/10.1016/j.sedgeo.2007.12.002>.
- León Canales, J., Vicuña del Río, M., Gubler, A., 2019. Increasing tsunami risk through intensive urban densification in metropolitan areas: A longitudinal analysis in Viña del Mar, Chile. *Int. J. Disast. Risk Reduct.* 41, 101312 <https://doi.org/10.1016/j.ijdrr.2019.101312>.
- León, T., Vargas, G., Salazar, D., Goff, J., Guendon, J.L., Andrade, P., Alvarez, G., 2019. Geo-archaeological records of large Holocene tsunamis along the hyperarid coastal Atacama Desert in the major northern Chile seismic gap. *Quat. Sci. Rev.* 220, 335–358. <https://doi.org/10.1016/j.quascirev.2019.07.038>.
- Lockridge, P.A., 1985. Tsunamis in Peru-Chile: *The Center*.
- Lomnitz, C., 1970. Major earthquakes and tsunamis in Chile during the period 1535 to 1955. *Geol. Rundsch.* 59 (3), 938–960. <https://doi.org/10.1007/BF02042278>.
- Lomnitz, C., 2004. Major Earthquakes of Chile: a Historical Survey, 1535–1960. *Seismol. Res. Lett.* 75 (3), 368–378. <https://doi.org/10.1785/gssrl.75.3.368>.
- Mather, A.E., Hartley, A.J., Griffiths, J.S., 2014. The giant coastal landslides of Northern Chile: Tectonic and climate interactions on a classic convergent plate margin. *Earth Planet. Sci. Lett.* 388, 249–256.
- May, S., Pint, A., Rixhon, G., Kellat, D., Wennrich, V., Brückner, H., 2013. Holocene coastal stratigraphy, coastal changes and potential palaeoseismological implications inferred from geo-archives in Central Chile (29–32° S). *Zeitschrift für Geomorphologie Supplementary Issues* 57, 201–228. <https://doi.org/10.1127/0372-8854/2013/S-00154>.
- McAdoo, B.G., Friitz, H.M., Jackson, K.L., Kalligeris, N., Kruger, J., Bonte-Graptent, M., Moore, A.L., Rafiaou, W.B., Bill, D., Tiano, B., 2008. Solomon Islands Tsunami, One year later. *Eos* 89 (18), 169–170. <https://doi.org/10.1029/2008EO180001>.
- Ministerio de Obras Publicas, 2015. Atlas del Agua Chile, p. 2016.
- Monge, J., Mendoza, J., 1993. Study of the effects of tsunami on the coastal cities of the region of Tarapacá, north Chile. *Tectonophysics* 218 (1), 237–246. [https://doi.org/10.1016/0040-1951\(93\)90270-T](https://doi.org/10.1016/0040-1951(93)90270-T).
- Moreno, M., Melnick, D., Rosenau, M., Bolte, J., Klotz, J., Echter, H., Baez, J., Bataille, K., Chen, J., Bevis, M., Hase, H., Oncken, O., 2011. Heterogeneous plate locking in the South-Central Chile subduction zone: building up the next great earthquake. *Earth Planet. Sci. Lett.* 305 (3), 413–424. <https://doi.org/10.1016/j.epsl.2011.03.025>.
- Morton, R.A., Gelfenbaum, G., Buckley, M.L., Richmond, B.M., 2011. Geological effects and implications of the 2010 tsunami along the central coast of Chile. *Sediment. Geol.* 242 (1–4), 34–51. <https://doi.org/10.1016/j.sedgeo.2011.09.004>.
- Muñoz Cupitty, D., 2019. Geoaqueología de tsunamis históricos en la costa hiperarida de Arica y Parinacota. (Bachelor). Universidad de Chile.
- Muñoz Cupitty, D., Easton, G., Goff, J., Salazar, D., González, G., Andrade, P., González-Alfaro, J. and León, T. (unpublished results). Geo-archaeological records of Historic tsunamis in the coast of Arica and Parinacota.
- Nakanishi, R., Ashi, J., 2022. Sediment transport modeling based on geological data for Holocene coastal evolution: wave source estimation of sandy layers on the Coast of Hidaka, Hokkaido, Japan. *J. Geophys. Res. Earth Surf.* 127 (8) <https://doi.org/10.1029/2022JF0066721> e2022JF0066721.
- Namegaya, Y., Yata, T., 2014. Tsunamis which affected the Pacific Coast of Eastern Japan in medieval times inferred from historical documents. *Zisin (J. Seismol. Soc. Japan. 2nd ser.)* 66, 73–81. <https://doi.org/10.4294/zisin.66.73>.
- Naranjo, J., Arenas, M., Clavero, J., Muñoz, O., 2009. Mass movement-induced tsunamis: Main effects during the Patagonian Fjordland seismic crisis in Aisén (45°25' S), Chile. *Andean Geol. - ANDEAN GEOL.* 36. <https://doi.org/10.4067/S0718-71062009000100011>.
- National Oceanic and Atmospheric Administration, 2022. National Geophysical Data Center/World Data Service: NCEI/WDS Global Historical Tsunami Database.
- Nelson, A.R., Kashima, K., Bradley, L.A., 2009. Fragmentary evidence of great-earthquake subsidence during Holocene emergence, Valdivia Estuary, South Central Chile. *Bull. Seismol. Soc. Am.* 99 (1), 71–86. <https://doi.org/10.1785/0120080103>.
- Nentwig, V., Tsukamoto, S., Frechen, M., Bahlburg, H., 2015. Reconstructing the tsunami record in Tirúa, Central Chile beyond the historical record with quartz-based SAR-OSL. *Quat. Geochronol.* 30, 299–305. <https://doi.org/10.1016/j.quageo.2015.05.020>.
- Nentwig, V., Bahlburg, H., Górecka, E., Huber, B., Bellanova, P., Witkowski, A., Encinas, A., 2018. Multiproxy analysis of tsunami deposits—the Tirúa example, central Chile. *Geosphere* 14 (3), 1067–1086. <https://doi.org/10.1130/ges01528.1>.
- Nichol, S., Lian, O.B., Carter, C.H., 2003. Sheet-gravel evidence for a late Holocene tsunami run-up on beach dunes, Great Barrier Island, New Zealand. *Sediment. Geol.* 155 (1–2), 129–145.
- NOAA, 2021. National Geophysical Data Center / World Data Service: NCEI/WDS Global Historical Tsunami Database.
- Okal, E., 2010. Tsunamiogenic earthquakes: past and present milestones. *Pure Appl. Geophys.* 168, 969–995. <https://doi.org/10.1007/s00024-010-0215-9>.
- Paskoff, R., 1991. Likely occurrence of a mega-tsunami in the middle Pleistocene, near Coquimbo, Chile.
- Peel, M.C., Finlayson, B.L., A., M. T., 2007. Updated world map of the Köppen-Geiger climate classification. *Hydrol. Earth Syst. Sci.* 11, 12.
- Ramírez, D., 1988. Estimación de algunos parámetros focales de grandes terremotos históricos y chilenos. MSc thesis. Universidad de Chile.
- Riou, B., Chaumillon, E., Chague, C., Sabatier, P., Schneider, J.L., Walsh, J.P., Zawadzki, A., Fierro, D., 2020. Backwash sediment record of the 2009 South Pacific Tsunami and 1960 Great Chilean Earthquake Tsunami. *Sci. Rep.* 10 (1), 4149. <https://doi.org/10.1038/s41598-020-60746-4>.
- Robinson, C.K., Wierzbos, J., Black, C., Crits-Christoph, A., Ma, B., Ravel, J., Ascaso, C., Artieda, O., Valea, S., Roldán, M., 2015. Microbial diversity and the presence of algae in halite endolithic communities are correlated to atmospheric moisture in the hyper-arid zone of the Atacama Desert. *Environ. Microbiol.* 17 (2), 299–315.
- Ruiz, S., Madariaga, R., 2018. Historical and recent large megathrust earthquakes in Chile. *Tectonophysics* 733, 37–56. <https://doi.org/10.1016/j.tecto.2018.01.015>.
- Russo, R., Gallego, A., Comte, D., Mocanu, V.I., Murdie, R.E., Mora, C., VanDecar, J.C., 2011. Triggered seismic activity in the Liquiñe-Ofqui fault zone, southern Chile, during the 2007 Aysen seismic swarm. *Geophys. J. Int.* 184 (3), 1317–1326.
- Salazar, D., Easton, G., Goff, J., Guendon, J.L., González-Alfaro, J., Andrade, P., Villagrán, X., Fuentes, M., León, T., Abad, M., Izquierdo, T., Power, X., Sitzia, L., Álvarez, G., Villalobos, A., Olgún, L., Yrarrázaval, S., González, G., Flores, C., Borie, C., Castro, V., Campos, J., 2022. Did a 3800-year-old Mw ~9.5 earthquake trigger major social disruption in the Atacama Desert? *Science. Advances* 8 (14), eabm2996. <https://doi.org/10.1126/sciadv.abm2996>.
- Satake, K., Heidarzadeh, M., Quiroz, M., Cienfuegos, R., 2020. History and features of trans-oceanic tsunamis and implications for paleo-tsunami studies. *Earth Sci. Rev.* 202 <https://doi.org/10.1016/j.earscirev.2020.103112>.
- Sawai, Y., Namegaya, Y., Okamura, Y., Satake, K., Shishikura, M., 2012. Challenges of anticipating the 2011 Tohoku earthquake and tsunami using coastal geology. *Geophys. Res. Lett.* 39 (21).
- Schurr, B., Asch, G., Hainzl, S., Bedford, J., Hoegner, A., Palo, M., Wang, R., Moreno, M., Bartsch, M., Zhang, Y., Oncken, O., Tilmann, F., Dahm, T., Victor, P., Barrientos, S., Vilotte, J.-P., 2014. Gradual unlocking of plate boundary controlled

- initiation of the 2014 Iquique earthquake. *Nature* 512 (7514), 299–302. <https://doi.org/10.1038/nature13681>.
- Sepúlveda, S.A., Serey, A., Lara, M., Pavez, A., Rebolledo, S., 2010. Landslides induced by the April 2007 Aysén fjord earthquake, Chilean Patagonia. *Landslides* 7 (4), 483–492.
- SHOA, S.H., de la Armada, O., 2010. Registro de los principales Tsunamis que han afectado a la costa de Chile. *Santiago*.
- Shuto, N., Fujima, K., 2009. A short history of tsunami research and countermeasures in Japan. *Proc. Japan Acad. Ser. B* 85 (8), 267–275.
- Soloviev, S.L., 1984. Catalogue of Tsunamis on the Western Shore of the Pacific Ocean: Institute of Oceanic Sciences, Canada.
- Spiske, M., Bahlburg, H., 2011. A quasi-experimental setting of coarse clast transport by the 2010 Chile tsunami (Bucalemu, Central Chile). *Mar. Geol.* 289 (1–4), 72–85. <https://doi.org/10.1016/j.margeo.2011.09.00>.
- Spiske, M., Piepenbreier, J., Benavente, C., Bahlburg, H., 2013a. Preservation potential of tsunami deposits on arid siliciclastic coasts. *Earth Sci. Rev.* 126, 58–73. <https://doi.org/10.1016/j.earscirev.2013.07.009>.
- Spiske, M., Piepenbreier, J., Benavente, C., Kunz, A., Bahlburg, H., Steffahn, J., 2013b. Historical tsunami deposits in Peru: sedimentology, inverse modeling and optically stimulated luminescence dating. *Quat. Int.* 305, 31–44. <https://doi.org/10.1016/j.quaint.2013.02.010>.
- Spiske, M., Bahlburg, H., Weiss, R., 2014. Pliocene mass failure deposits mistaken as submarine tsunami backwash sediments — an example from Hornitos, northern Chile. *Sediment. Geol.* 305, 69–82. <https://doi.org/10.1016/j.sedgeo.2014.03.003>.
- Spiske, M., Tang, H., Bahlburg, H., 2020. Post-depositional alteration of onshore tsunami deposits – Implications for the reconstruction of past events. *Earth Sci. Rev.* 202, 103068 <https://doi.org/10.1016/j.earscirev.2019.103068>.
- Stewart, D., 2019. Historical tsunamis in the Concepcion bay, as seen in the reconstructed flood levels from the colonial city of Concepcion (Penco), Chile (1570–1835). *Revista de historia (Concepción)* 26, 97–127. <https://doi.org/10.4067/S0717-88322019000200097>.
- Sugawara, D., Yu, N.T., Yen, J.Y., 2019. Estimating a tsunami source by sediment transport modeling: a primary attempt on a historical/1867 normal-faulting tsunami in Northern Taiwan. *J. Geophys. Res. Earth Surf.* 124 (7), 1675–1700. <https://doi.org/10.1029/2018jf004831>.
- Szczuciński, W., 2012. The post-depositional changes of the onshore 2004 tsunami deposits on the Andaman Sea coast of Thailand. *Nat. Hazards* 60 (1), 115–133.
- Szczuciński, W., Niedzielski, P., Rachlewicz, G., Sobczyński, T., Ziota, A., Kowalski, A., Lorenc, S., Siepak, J., 2005. Contamination of tsunami sediments in a coastal zone inundated by the 26 December 2004 tsunami in Thailand. *Environ. Geol.* 49 (2), 321–331.
- Szczuciński, W., Niedzielski, P., Kozak, L., Frankowski, M., Ziota, A., Lorenc, S., 2007. Effects of rainy season on mobilization of contaminants from tsunami deposits left in a coastal zone of Thailand by the 26 December 2004 tsunami. *Environ. Geol.* 53 (2), 253–264.
- Tsuji, Y., 2013. Catalog of distant Tsunamis reaching Japan from Chile and Peru. *Rep. tsunami Eng.* 30, 8.
- Udias, A., Madariaga, R., Buforn, E., Muñoz, D., Ros, M., 2012. The Large Chilean Historical Earthquakes of 1647, 1657, 1730, and 1751 from contemporary documents. *Bull. Seismol. Soc. Am.* 102, 1639–1653. <https://doi.org/10.1785/0120110289>.
- Vargas, G., Ortlieb, L., Chapron, E., Valdes, J., Marquardt, C., 2005. Paleoseismic inferences from a high-resolution marine sedimentary record in northern Chile (23°S). *Tectonophysics* 399 (1–4), 381–398. <https://doi.org/10.1016/j.tecto.2004.12.031>.
- Vargas, G., Farias, M., Carretier, S., Tassara, A., Baize, S., Melnick, D., 2011. Coastal uplift and tsunami effect associated to the 2010 Mw 8.8 Maule earthquake in central Chile. *Andean Geol.* 38, 21.
- Watt, S.F., Pyle, D.M., Naranjo, J.A., Mather, T.A., 2009. Landslide and tsunami hazard at Yate volcano, Chile as an example of edifice destruction on strike-slip fault zones. *Bull. Volcanol.* 71 (5), 559–574.
- Weiss, R., Lynett, P., Wünnemann, K., 2015. The Eltanin impact and its tsunami along the coast of South America: insights for potential deposits. *Earth Planet. Sci. Lett.* 409, 175–181.
- Yamada, M., Fujino, S., Goto, K., 2014. Deposition of sediments of diverse sizes by the 2011 Tohoku-oki tsunami at Miyako City, Japan. *Mar. Geol.* 358, 67–78. <https://doi.org/10.1016/j.margeo.2014.05.019>.
- Yoshii, T., Imamura, M., Matsuyama, M., Koshimura, S., Matsuoka, M., Mas, E., Jimenez, C., 2012. Salinity in Soils and Tsunami deposits in areas affected by the 2010 Chile and 2011 Japan tsunamis. *Pure Appl. Geophys.* 170 (6–8), 1047–1066. <https://doi.org/10.1007/s00024-012-0530-4>.